Materials Aspects of Photonic Crystals**

By *Cefe López**

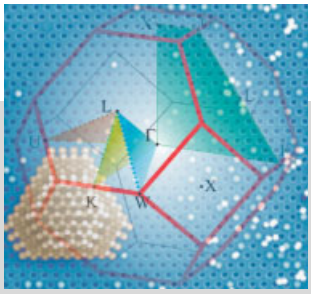

Photonics, the technology of photons (as electronics is the technology of electrons), promises to be the new century's driving force in the advancement of, mainly but not only, information technology, such as communications and computing. This technology was initiated with the advent of lasers and optical fibers that, for various reasons, embody the best choice of source and channel of the information carrier: the photon. If the parallel with electronics is to be further pursued, one soon realizes that many more components are needed not only in the transport section of the technology but also, and principally, in the logic section: signal processing. An answer is promised to many of these demands by the potentiality of the new photonics era: photonic bandgap (PBG) materials, otherwise known as photonic crystals (PCs). In the present review a general perspective is presented on the state of the art in PC technology providing a broad audience-oriented description of fundamentals and properties.

1. Introduction

Although it seems that most of the notions relating to photonic crystals (PCs) are rooted in basic solid-state physics concepts and are, then, well known, it is worth pointing out that they were originally borrowed by solid-state physics from the theory of electromagnetism and are, thus, returning to their source. Although the concepts are well known we must concede that there is still a long way to go in the materials aspects of the problem. This imposes a clear need for the focus of this compilation. Furthermore, we must also admit that, among the approaches to the problem, the ones involving more materials issues and unknowns are the three-dimensional (3D) PCs and the production methods other than those adopted from microelectronics—very much two-dimensional (2D) technologies. For their idiosyncratic nature, colloidal systems lend themselves to be used as natural starting points for the purpose of creating and using PCs, and, as such, occupy an important place in current research in this field. In their exploitation and characterization, a broad range of techniques and different sources of knowledge contribute, and the interdisciplinary nature of the subject further enriches it. The review is thus oriented to an audience of physicists, chemists, engineers, etc. and tries to bring together concepts from various fields for the benefit of the widest possible audience. For instance, due to their inherent porosity, these materials, and the techniques involved, attract interest from other areas such as catalysis, templating other materials, etc. A whole wealth of materials properties are involved, which spring from their architectural scale. From the molecular level, and up to the macroscopic structure, micro- and mesoscopic regimes involve new properties, processes, and phenomena, like synthesis in new environments, mechanical, optical, electronic, magnetic, etc.

In his seminal paper of 1987 Yablonovitch[1] sensed that "further materials development" might be required before the benefits of spontaneous emission inhibition were fully felt. Likewise, John[2] suggested some materials that, based upon their refractive index (RI), could provide a test-bed for the study of strong localization of light. These two very different approaches to a common subject revealed a consciousness of the materials aspects in basic science. A huge effort has since been devoted to developing materials and structures that could support and expand their initial hypotheses. Besides, because RI contrast is a key issue in this class of structures, a materials controversy arises because higher RI materials provide better photonic bandgap (PBG) performance, but at the same time impose higher scattering rates and, hence, losses.

In this paper, a review of recent developments in PCs will be given, paying special attention to the materials aspects but giving a general overview of the field. The paper is structured as follows. This section serves as introduction of the basics, aims, and applications. It will also deal with the main techniques of characterization, namely, optical spectroscopy and its fundamentals, and with the interpretation of results in terms of photonic band structure. Section 2 is devoted to fabrication techniques reviewing different methods and leaving the self-assembly approach, comprising synthesis of nano- and micro-particles, assembly thereof, and posterior treatments,

[*] Dr. C. López
Instituto de Ciencia de Materiales de Madrid (CSIC)
Cantoblanco, 28049-Madrid (Spain)
E-mail: cefe@icmm.csic.es

[**] This work was partially financially supported by the Spanish CICyT contract MAT2000–1670-C04. The author is indebted to numerous people for valuable discussions and suggestions, among which the members of the PCs group in ICMM and former collaborators (F. Meseguer and J. Sánchez-Dehesa foremost) are to be counted. The author is also indebted to and acknowledges J. D. McCulloch for thorough proofreading.

 DOI: 10.1002/adma.200300386

for Section 3. The latter includes a summary of various composites that can be produced using opals as templates. Inverse structures resulting from the removal of the opal backbone are described with special emphasis on those materials with the highest dielectric constant.

1.1. PBG Materials

Different approaches to a subject can illuminate and give a broader perspective. For that reason several methods of tackling the problem of scattering by periodic media are described.

1.1.1. Background

PBG materials, generally called PCs, are a class of materials or structures, rather, in which the dielectric function suffers a spatially periodic variation. Of course, the length scale in which the variation takes place (lattice parameter) determines the spectral range of functioning of the PC and, as a rule of thumb, the wavelength, at which the effects are felt corresponds approximately to the lattice parameter. This can be achieved by structuring a single compound, or by constructing a composite made up of homogeneous materials with different dielectric properties. Thus, a PC working in the optical range of the electromagnetic (EM) spectrum will present a modulation of the dielectric function with a period of the order of one micrometer, one designed for microwaves should be modulated with a period of some centimeters, and a PC for X-rays should present a modulation of some angstroms, which is a solid-state crystal. The most prominent feature of such structures is that they present iridescences as a result of diffraction. Some natural examples are the multilayered structure of pearls, the flashing wings of several insects,[3] and natural opals.[4] The same effect appears in familiar man-made objects such as compact disks.

When modeling the diffraction of light by a periodic medium (actually an atomic crystal) as a layered structure, one computes the phase difference accumulated by rays that suffer scattering from different planes in the stack and adds up those with a multiple of 2π (constructive interference). With a little more algebra this leads to Bragg's law. A similar approach yields the (equivalent) Laue formulation, and both give rise to the concept of reciprocal lattice. This is a lattice (in the wavevector space), all of whose points generate plane waves with the periodicity of the direct lattice. This simple formulation, as can be found in solid-state physics text books,[5] provides a description of the scattering properties of the periodic system in the form of sets of pairs (wavelength, direction) for which the light does not enter the structure, but, rather, is Bragg diffracted. For any given direction several orders of diffraction may be considered, inspiring the idea of various bands for a given wavevector.

The previous description is fairly well suited to the X-ray scattering for which it was initially developed. Its validity relies on the fact that the RI negligibly departs from unity, since the energy of the photons involved is immensely larger than the elementary excitations in the material (no absorption). If this approximation is to be adapted to the optical range, a model in which something more is said about the RI distribution is required.

The simplest such model might be a one-dimensional (1D) periodic variation of the dielectric function. Fourier expansions of periodic magnitudes become summations rather than integrals. These summations contain a discrete (though infinite) number of plane wave-like terms, each corresponding (not by chance) to a vector of the reciprocal lattice. The dielectric function can then be expanded in such a way, and so can all other periodic magnitudes involved. If introduced in a scalar wave equation, this leads to an expression for the wavevector as a function of energy. The interesting result is that, for certain energy ranges—marked as stripes in Figure 1—no purely real solutions exist and the wavevector has a non-vanishing imaginary part, which means that the wave suffers attenuation and does not propagate (at least not through an infinite crystal). The wavevector at which this happens is that predicted by Bragg's law, and the range of energies where $\boldsymbol{k}$ is no longer real (but complex) is called the stop band. One other interesting fact is that for this wavevector there are two solutions (energies): one above and one below the gap, both having the same periodicity but spatially shifted with respect to each other. The stop band width is mainly determined by the dielectric contrast: the greater the contrast, the wider the

Cefe López was born in Trelles, Spain, in 1961. He graduated in Physics in 1984 from the Universidad Autónoma de Madrid where he received a PhD in 1989. He spent two years at the University of Oxford and returned as assistant professor to the Universidad Carlos III, Madrid, where he taught Physics for two years. In 1993, he entered the Spanish Research Council (CSIC) where he is currently a Scientific Researcher. With expertise in optical spectroscopy and a background in the physics of semiconductors, his research interests are centered on wave crystals, more specifically photonic bandgap crystals. He heads a team in the Materials Science Institute of Madrid, whose research focuses on developing and investigating novel materials based on opals.

ADVANCED MATERIALS

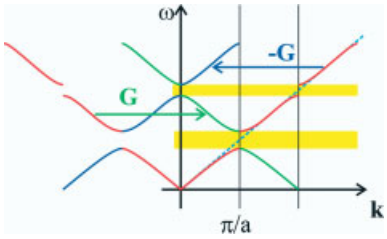

Fig. 1. Dispersion relation for a homogeneous material (light cyan dashed straight line) and for a periodic material with the same average RI and period *a*.

gap. It also explains that even infinite crystals will present a finite diffraction peak width as opposed to X-ray diffraction, where peak width ($\Delta\lambda/\lambda \sim 10^{-6}$) is mainly accounted for by crystal size broadening (Scherer's law). This very simple model can be further improved if we wish to consider the three dimensions.[6] If a single Fourier term in the expansion is assumed to dominate the sum close to a diffraction, simple expressions are obtained that account for the width of diffraction peaks for common structures fairly well.[7] Of course, the assumption that only one term in the summation is non-negligible limits the applicability to restricted energy ranges.

A parallel with the molecular orbital approach can also be established. If we think of the tiles composing a PC as optical atoms where (Mie) resonances can exist we can draw a picture in which a band structure is built from single states. Let us start with one scatterer (atom) and let us concentrate on one of its resonances. If two such atoms approach one another, they will eventually start interacting, and their resonances will split and produce two new common states (molecular orbitals). If more and more atoms are added in an ordered fashion, new states will be produced, and bands of tightly packed states will emerge. If the atoms are arrayed in a periodic fashion, translational symmetry will provide a quantum number to label the states: the $\boldsymbol{k}$ wavevector. The various resonances give rise to various bands, like in semiconductor physics the different atomic orbitals give rise to different bands in the solid.[8] Of course, interaction between states dilutes the initial character of the optical resonance.

So far, we have only described the EM field as a scalar wave. Additionally, only a single reciprocal lattice vector has been taken into account at a time in the Fourier expansions. A more rigorous treatment is then required that accounts also for all possible effects associated with the vectorial character of EM radiation. This was done for the first time by expanding the EM fields in plane waves and solving the Maxwell equation exactly—no approximations assumed—in a numerical fashion for periodic arrangements of spherical atoms in face centered cubic (fcc)[9] and diamond lattices.[10]

After a little manipulation, Maxwell equations can be reduced to a wave equation of the form:

$$\nabla \times \left[\frac{1}{\varepsilon(\boldsymbol{r})}\nabla \times \boldsymbol{H}(\boldsymbol{r})\right] = \frac{\omega^2}{c^2}\boldsymbol{H}(\boldsymbol{r}) \qquad (1)$$

which is an eigenvalue problem for $\boldsymbol{H}(\boldsymbol{r})$, the magnetic field. It can be shown that the operator acting on the $\boldsymbol{H}(\boldsymbol{r})$ field ($\Theta = \nabla \times 1/\varepsilon(\boldsymbol{r}) \times$) is Hermitian, and, as a consequence, its eigenvalues are real and positive. These are the very properties of a Hamiltonian in quantum mechanics that offer the possibility to derive many properties therefrom and think of PCs in solid-state physics terms. A more detailed description can be found in the book by J. D. Joannopoulos et al.[11] Since $\varepsilon(\boldsymbol{r})$ is periodic, we can use Block's theorem; we also expand all fields in plane waves. After some more algebra, this equation is reduced to a matrix diagonalization problem, whose eigenvalues are the photonic bands, that is, lists of pairs of the kind $(\omega, \boldsymbol{k})_n$ that can be viewed as successions (labeled by n) of energies ω for every wavevector $\boldsymbol{k}$, or series of functions $\omega_n(\boldsymbol{k})$. It is particularly important to realize that this wavevector $\boldsymbol{k}$ can be (and is often) confined (in plotting band diagrams) to the first Brillouin zone (BZ): a region of reciprocal space closer to the origin than to any other reciprocal lattice point. This is schematically depicted in Figure 1, where energy dispersion is folded back into the BZ by subtracting some reciprocal lattice vector. The EM energy is proportional to the dielectric function and the electric field squared, thus accounting for a difference in energy despite a similar distribution of electric field. An EM field stores more energy if it has extrema (rather than nodes) at the regions of higher dielectric function so that lower energy states concentrate in high dielectric function regions.[12] It should also be pointed out that the periodicity of the system transforms the wavevector (or momentum for that matter) conservation rule into a requirement that, in a scattering process, the wavevector must change by a reciprocal lattice vector $\boldsymbol{G}$. This acquires importance when analyzing scattering processes, where momentum must be conserved and, thus, incoming, $\boldsymbol{k}_{\text{in}}$, and outgoing, $\boldsymbol{k}_{\text{out}}$, momenta must satisfy $\boldsymbol{k}_{\text{out}} - \boldsymbol{k}_{\text{in}} = \boldsymbol{G}$. Eventually, this may reduce to the ordinary $\boldsymbol{k}_{\text{out}} = \boldsymbol{k}_{\text{in}}$ for $\boldsymbol{G} = 0$.

This is universally acknowledged to be the correct description of the photon states in a periodic medium. It is soon realized that, in these systems, much more restrictive conditions for gap appearance are faced than in the case of electrons in solids.[13] There is yet another subtle difference, in that for photons there is no length scale involved as a Bohr radius. This lack of an absolute length scale makes the physics of PCs scalable: resizing the system resizes the energy in such a way that the spectrum in units of c/*a* independent of size (c being the speed of light and *a* the system lattice parameter). Since $\omega/(2\pi c/a) = a/\lambda$, it is customary to use such units to measure the energy. Besides the scalability in space there is a scalability in dielectric function: there is no fundamental scale for ε. Two systems whose dielectric functions scale by a factor, $\varepsilon'(\boldsymbol{r}) = \varepsilon(\boldsymbol{r})/s^2$ have spectra scaled by the same factor: $\omega' = s\omega$, which means that increasing the dielectric function by four decreases the energies by two.

The foregoing analysis can be summarized by saying that the propagation of waves in periodic media is peculiar in that it breaks the otherwise linear dispersion relationship into bands (of propagating waves) and gaps (where propagation is forbidden).

Periodicity can be made to occur in one, two, or three directions. Most of the properties discussed so far are independent of

dimensionality and are well exemplified by sticking to 1D systems. Such systems, extensively used in optical applications, are called Bragg reflectors, and consist of stacks of alternating high and low RI transparent materials that base their superiority over metallic mirrors on their reflectance without dissipation.

There are however certain aspects that might require some inspection when more dimensions are considered. 2D systems are used more and more often for micro-photonic applications and consist of periodic repetitions of objects in a 2D arrangement, like, for instance, rods periodically arranged parallel to one another. In this case, the dielectric function varies periodically in a plane perpendicular to the rods' axes but it is independent of the position along the axis. 3D systems present a modulation in the third direction, like in a stack of spheres. Since the energy spectrum is directionally dependent, a gap found in one direction will not be a real gap if there are states in other directions within this energy.

1.1.2. The Band Structure

Let us now turn to some aspects of the band structure that will help in interpreting optical spectra later on. For this, good starting points are introductory solid-state physics text books and specialized sources, such as the book by K. Sakoda,[14] but we shall summarize the most important results.

A typical 3D dispersion diagram is shown in Figure 2. The x-axis represents momentum and the y-axis represents energy measured in very convenient adimensional units: a/λ, where a is the lattice parameter. The different panels composing the diagram represent paths between important (high symmetry) points (labeled X, U, L, etc.) in reciprocal space, which (not by chance) happen to be the midpoints of the segments joining the origin to its nearest neighbors in the reciprocal lattice, and thus represent propagation directions.

Panels starting at Γ, e.g., ΓX, show the dispersion relation for states with increasing $\boldsymbol{k}$, all pointing in the same direction (X = (001)), whereas in panels such as XW both direction and modulus of $\boldsymbol{k}$ vary continuously to sweep from X to W.

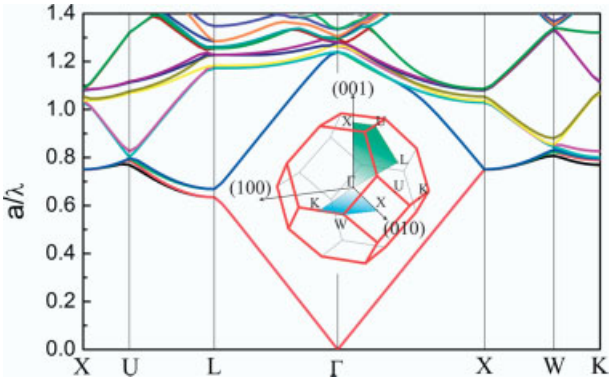

Fig. 2. Dispersion relation for a PC made of silica spheres in a compact fcc. For these structures the lattice parameter is given by $a = \sqrt{2}D$, where D is the sphere diameter. Owing to the scalability of the theory, the band diagram is independent of the lattice parameter (and, thus, of sphere size) so long as the dielectric function is not dispersive. Therefore, any such structure can be modeled by a single band diagram.

Among the many bands that are seen in the ΓL panel, some have the ordinary $\omega = (c/n)k$ form (n being an effective RI) or $\omega = (c/n)(k–2\pi/a)$, resulting from shifting such a relation by one reciprocal lattice vector parallel to the vector involved. This is shown in Figure 1 as a translation of the red curve by $2\pi/a$.[15] There are other curves that result from the folding back into the BZ by means of vectors not parallel to the ΓX direction, as depicted in Figure 3. These bands have an expression like $\omega = (c/n)k' = (c/n)[(2\pi/a)^2 + k^2]^{1/2}$, which makes

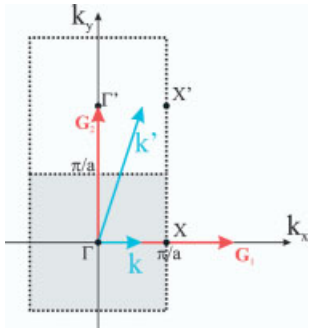

Fig. 3. An arbitrary wavevector, $\boldsymbol{k}'$, is folded back into the first BZ, $\boldsymbol{k}$, by subtracting the closest reciprocal lattice vector ($\boldsymbol{G}_2$).

them less dispersive. This picture gets even more complicated for 3D, where many more vectors are involved, and is only simplified by symmetry properties making the bands degenerate. Of course, this degeneracy may be lifted, for instance, by a slight deformation.

Looking at the bands in any panel in Figure 2, it can be seen that not all energies are covered by the bands. The regions where bands leave unfilled spaces are the gaps. Looking at the whole diagram, we can see that none of these gaps are present for every wavevector: there are no complete gaps. As mentioned before, RI contrast enhances the width of the gaps. If we could continuously tune the contrast down to a homogeneous medium (of any RI) the bands would evolve to a situation where no gaps would be left and bands would cover the whole spectrum. This can be expressed by saying that larger Fourier coefficients lead to larger gaps, and Fourier coefficients are synonymous to strong modulation. Gap widths are governed by refractive contrast, while gap positions are governed by average RI. However, the existence of complete gaps very strongly depends also on the topology. Gaps found in different directions occur at different energies. This can be roughly explained as follows. Gaps open at the edges of the BZ located at $k = \pi/d$, where d is the periodicity in that direction. The corresponding energy is ck/n so that, if a structure presents very different periodicities in different directions, the gaps will open at very different energies and will hardly overlap. The lattice alone does not determine the band structure: the shape of the "atoms" also plays an important role; as suggested above, the symmetry of the cell may lift degeneracies that eventually can open gaps. The best chances to find a structure with a complete gap are for lattices with a BZ that is as round as possible and a primitive cell with non-spherical

ADVANCED MATERIALS

atoms inside. In 3D, this points towards the fcc lattice,[16] a particular case of which is the diamond lattice, where each lattice site contains two atoms.

When bands depart form the "free photon" behavior $\omega = ck/n$, the RI must be taken as $n = c/(\mathrm{d}\omega/\mathrm{d}k)$ rather than $n = ck/\omega$, and very peculiar behaviors can be obtained. The group (or energy transmission) velocity, the only meaningful one in these systems, is now $v_g = \mathrm{d}\omega/\mathrm{d}k$ rather than $v = \omega/k$. Near the center and edges of the BZ, bands flatten out and group velocities tend to zero. The net effect is that the time taken by the EM field to traverse the sample is dramatically increased enhancing the interaction between light and matter. Since, for multidimensional systems, the derivative is actually a gradient, the correct expression for the velocity in the nth band is

$$\mathbf{v}_n(\boldsymbol{k}) = \nabla_{\boldsymbol{k}}\omega_n(\boldsymbol{k}) \tag{2}$$

which means that propagation is (as the gradient) normal to equi-energy surfaces. Equi-energy surfaces cross Bragg planes at right angles. These and other concepts are best examined in a solid-state physics text book.[17]

For wave-vectors near or beyond the first BZ equi-energy surfaces cross many Bragg planes and are strongly distorted from the free photon (uniform medium) spherical shape. We can visualize it by taking horizontal sections in Figure 2 and seeing that different $\boldsymbol{k}$s are required to cross a band if searching in different directions. This has important consequences, because, in this situation, the propagation direction may differ greatly from the wavevector as shown in Figure 4. If the energy is changed the surface will also change shape with the corresponding change in propagation direction. At some points, this change may be rapid with the associated swing in direction for small changes in energy, and the system may be used to separate frequencies.

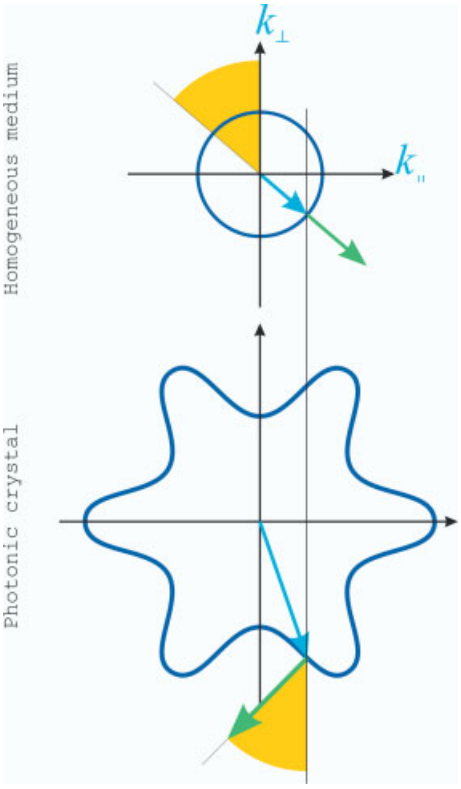

Fig. 4. In homogeneous media, equi-energy surfaces are spherical, $\omega = c\,|\boldsymbol{k}|/n$, and propagation (green) direction and wavevector (blue) are collinear. But in PCs these surfaces become very anisotropic. Conservation of the parallel component of the wavevector leads to very peculiar refraction effects since propagation is no longer collinear with the wavevector.

1.1.3. Phenomena in a PBG

In the presence of a PBG many new phenomena can be expected. They are brought about by the two main features of the band structure: the suppression of the density of states (DOS) and the translational symmetry.

Control of spontaneous emission in photonic systems through the photonic DOS was the primary goal in the first proposal of PBGs.[1] Spontaneous photon emission is genuinely quantum mechanical as vacuum fluctuations are at the heart of the phenomenon.[18] The rate of radiation of a dipole, according to the Fermi golden rule, is proportional to the density of final states. For an excited atom in vacuum this is the density of EM states at the energy of the excited state. So, if this DOS is suppressed, as in a PBG, no radiation is expected from the dipole, vacuum fluctuations are disabled, and the atom must remain in the excited state. The actual picture is that of a dressed atom,[19] formed as the bound state between the atom and the emitted photon, the energy bouncing back and forth between the atom and the EM field, giving rise to a Rabi splitting. When the leading part of the photon–atom interaction (spontaneous emission) is suppressed, the next process (resonance dipole–dipole interaction) needs to be considered. If emission occurs near a band edge, where the DOS jumps abruptly and Fermi's golden rule fails to describe the process, the system shows a large differential gain.

The alternative approach to PBGs was made bearing in mind localization.[2] As in semiconductor physics, a defect in an otherwise perfect crystal introduces a state in the gap with a localized wavefunction. The state must be in the gap where no extended states exist. This is because if the energy of the localized mode coincided with that of a Block (extended) state they would interact and the mixed wavefunctions, being combinations of localized and extended states, could not be localized. A mode of the EM field with its energy in the gap will remain confined in the vicinity of the defect since propagation is forbidden through the walls of the cavity. The magnitude describing the confining power of the defect is the quality, Q, that measures the rate of escape from the cavity, something like the number of oscillations of the mode before escape. It can also be expressed as the spectral width, $\Delta\omega/\omega$, of the state and directly relates to the decaying of the wave function into the PC: the more rapid the decay, the less interaction (narrower state) and smaller coupling with extended states (smaller probability of tunneling). High Q cavities are required to make low threshold lasers because they make bet-

ter use of the pump energy. However, a compromise must be achieved to have efficient power extraction.

The approximation that the polarization of a medium is proportional to the electric field breaks down for very intense fields, and we enter the realm of nonlinear optics. For these processes to take place, light–matter interaction is required, vacuum being linear. A typical example is second-harmonic generation. These processes can be classified as parametric (when the final state of the atom involved is unaltered) or non-parametric (if a change in the level population is produced) and are given an order according to the number of terms considered in the polarization power expansion. Second-harmonic generation is second-order nonlinearity, whereas intensity dependent RI is a third-order process. Here PCs are useful for various reasons. Since very high fields are needed PC microcavities provide the right tool to confine EM radiation in small volumes. The control over group velocity (down to very small values) with the corresponding enhancement of light–matter interaction favors the onset of nonlinear interactions. As in any other scattering event, conservation of energy and momentum (phase matching) must be considered. However, in PCs momentum must be conserved to a reciprocal lattice vector, which considerably relaxes the condition. Finally, symmetry considerations regarding the PC lattice must be taken into account that add to those relating to the atomic crystal symmetry of the host material.

1.2. Optical Characterization

The main technique for the characterization of PBG materials is, naturally, optical. Bragg diffraction is the primary feature of these systems and can be used for initial characterization. An interpretation in terms of bands is however most appropriate.

When RI contrast is low it is a good approximation to use ordinary diffraction or dynamic diffraction theory to characterize PCs. For this, small-angle X-ray scattering is an appropriate technique if a 2D detector is used.[20]

1.2.1. Reflectance and Transmission

Optical reflectance and transmission are the principal tools used to characterize 3D systems. In a reflectance experiment, a high-symmetry facet of the PC is often chosen. This places the normal in a high-symmetry direction in reciprocal space. Light is shone with $\boldsymbol{k}_i$ forming a given angle with the normal, and detected in specular configuration, that is, $\boldsymbol{k}_o$ in the incidence plane and forming the same angle with the normal. Energy is then scanned. Typical examples are shown in Figure 5. The two conditions to be satisfied are energy conservation, which requires that incident and reflected wavevector lie on a circle centered at the origin, and momentum conservation, which is granted by requiring that the tips of $\boldsymbol{k}_i$ and $\boldsymbol{k}_o$ be joined by some reciprocal lattice vector, $\boldsymbol{G}$. The darker hexagon represents the first BZ, the normal is defined by the direction ΓX and the red arrows are two reciprocal lattice vectors. In Figure 5a, reflection occurs at the X point (normal incidence); the incident and reflected beams travel in opposite directions. Spectra can be taken by varying the angle between $\boldsymbol{k}_i$ and the normal. If we increase the energy of the incident photon slightly the conditions can only be satisfied by tilting the incidence angle as in Figure 5b. Further increase may give rise to a situation where two scattering mechanisms are possible as in Figure 5c.

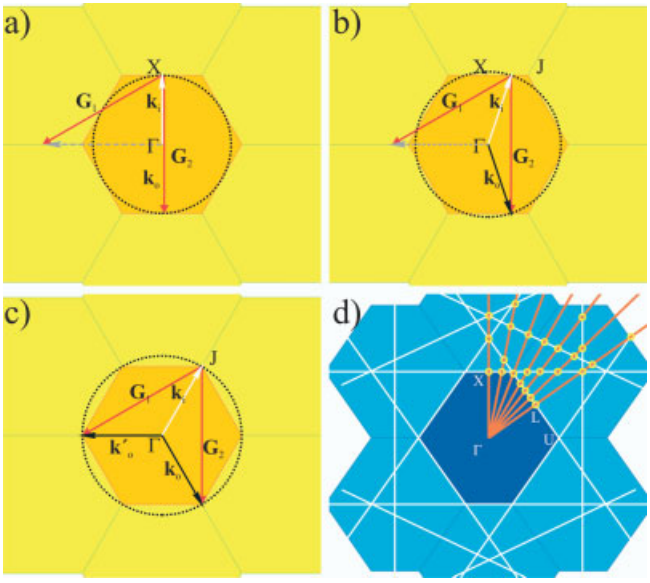

Fig. 5. Scattering diagram in reciprocal space: incident (scattered) wavevectors represented by white (black) arrows. For a nearly homogeneous medium, energy conservation is granted on the circular equi-energy surface. For vectors in gray, the energy is not conserved and the process is not allowed. In (d) Bragg planes other than those defining the first BZ are drawn, and Bragg diffractions are marked with yellow circles.

For transmission, the detector is placed in line behind the sample, and Bragg reflected photons are recorded as drops in transmitted intensity. At variance with the specular reflectance geometry, the transmission experiment does not select a Bragg plane because it does not rely on detecting the scattered photon but instead on detecting its absence. Thus, any scattering event, regardless of the direction of $\boldsymbol{k}_o$, will be recorded as a dip in intensity. Every Bragg plane crossed by $\boldsymbol{k}_i$ gives rise to a reflection as marked in Figure 5d with small circles. These diagrams give not only an idea of when a reflection can be expected to occur, but also where the scattered photon should be observed, although in transmission this is overlooked.

The preceding picture is valid for low RI contrast where the peaks are narrow, the interactions small, and the original character of the states preserved from those in the free-photon picture. When RI is high, equi-energy surfaces are no longer circular, this naïve picture breaks down, and a rigorous band structure calculation is required.

ADVANCED MATERIALS

1.2.2. Photonic Bands Interpretation

A full account of the interaction between PCs and light can only be given in terms of bands and gaps as described by a band structure diagram. As mentioned above the only meaningful wavevectors for states belonging to a PC are those contained in the first BZ. For a photon of energy ω, coming from outside, the wavevector, $\boldsymbol{k}'$, may have a modulus, k', larger than the BZ boundaries. Yet, for any phenomenon involving states of the PC, this photon will behave entirely as if its wavevector was $\boldsymbol{k} = \boldsymbol{k}' - \boldsymbol{G}$, such that $\boldsymbol{k}$ fits in the BZ for some $\boldsymbol{G}$ of the reciprocal lattice (see Fig. 3). These $\boldsymbol{G}$ vectors may or may not be parallel to $\boldsymbol{k}$, which will produce an interaction of external light with bands other than those originating from the folding of the nearly-homogeneous medium approximation (as in Fig. 1). In principle, a wave that impinges on a PC with a given energy and a $\boldsymbol{k}$ vector in a given direction is transmitted through the PC if a band is available in the dispersion diagram for the wavevector in the direction of $\boldsymbol{k}$. In Figure 6 (left) the bands diagram for $\boldsymbol{k} \parallel (111)$ is plotted. According to this diagram, photons incident in the (111) direction will be transmitted except for a narrow band (shaded area) around $a/\lambda \sim 0.65$, where no bands are available.

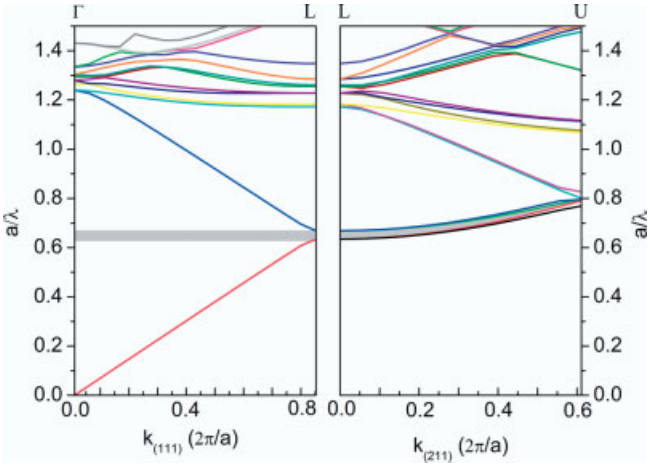

Fig. 6. Typical band dispersion for a bare opal for $\boldsymbol{k}$ parallel to the (111) direction (left) and for directions comprised between the (111) and (411). A gap is present at $a/\lambda \sim 0.65$ that shifts to higher energies upon changing direction. Bands with little or no dispersion can be seen at higher energies.

There may be circumstances when this picture is altered. Symmetry considerations[21] can impede coupling between the incoming EM field and the available state. If, for instance, the state has a mirror symmetry that the plane wave does not possess, overlap can vanish rendering the state useless for transmission. On the other hand, even when a band is available and the symmetry allows coupling with external waves the band may be such that the group velocity vanishes and transmission is virtually cancelled. This can be seen as a divergence of effective RI[22] with corresponding Fresnel reflectance approaching unity: $R = (n-1/n+1)^2 \sim 1$. The latter case usually occurs near the edges of the BZ, where it is often masked by real gaps, but it may also happen at intermediate $\boldsymbol{k}$s as in the upper bands in Figure 6.

The preceding remarks account for some more peaks appearing without the need for gaps at energies around 1.2. The analysis is very complicated because many bands intervene.[23] For any given frequency, propagation takes place by the contribution of many states that carry the energy in multiple directions. Only if the PC is a plane parallel slab, refractive phenomena at the entry facet will be reversed at the exit, restoring the fields to a collimated wave.

Searching the whole reciprocal space is required for a comprehensive characterization of the system, and this entails scanning in all directions. It is often enough, however, to scan the principal corners, defining the irreducible part of the BZ. The properties of lower symmetry points can be interpolated therefrom. The right panel in Figure 6 shows (shaded area) the evolution of the Bragg reflection highlighted on the left panel (gray rectangle) as the direction of propagation is changed. Here the abscissa is the wavevector component parallel to the LU segment. This is a typical example of an incomplete gap: the gap exists only for a certain direction, and as the direction is changed so does the position (and possibly its width).[24] If a gap, or at least some part of it, remained a gap for any direction of propagation a complete PBG would be found, and reflectance and transmission would present a feature for the corresponding range of energies.

If not only the energy but also the phase can be measured the real dispersion relation can be plotted. This involves very difficult techniques for optical frequencies but can be easily done in the microwave regime.[21]

1.2.3. Special Techniques

Very often 2D systems are built as very thin slabs where a periodic pattern is lithographically etched. Measuring the band dispersion diagram in such structures poses a challenge for experimental realization. Some approaches are described.

The direct method is, of course, feeding light from one end by means of a microscope objective or an optical fiber, and collecting it from the other end by similar means. Most often, the interest lies in characterizing waveguides (WGs), rather than the PC itself and, particularly, measuring losses. Losses have contributions from several mechanisms (insertion, radiation, scattering, etc.) and it is necessary to separate them.

When light is injected in a sample with its plane parallel to the front-rear facets, defined effective RI Fabry–Perot oscillations occur. The amplitude of the oscillations can be used to determine the reflectance of the facets (mirrors) and the attenuation in the medium. This technique can be used to characterize losses when the transmitting medium is a PC WG.[25] A reference channel is needed to measure the transmission through the WG. The particular property of the method is that it is independent of the coupling efficiency.

Inserting the light in the PC poses difficulties, and to avoid them an alternative method, producing the light inside, was realized. A quantum well placed in the center of the slab where the PC is fabricated acts as a source that can be excited

by a focused laser; light is collected from the side, in different orientations, by a microscope objective.[26]

In the surface coupling technique, light impinging on a 2D PC from outside couples with the 2D photonic structure if the component parallel to the surface and the energy match those of a state in the PC. This technique is, of course, limited to the part of (ω, $\boldsymbol{k}$) lying above the light line of the outside medium.[27] The relative orientation of the PC with respect to the plane of incidence determines the regions of the BZ explored. A similar method, relying on diffraction by the corrugated surface, has been applied for the determination of lattice parameters in colloidal crystals without any assumption of the RI.[28]

Near field optical microscopy is especially adequate for 2D systems but useful in 3D as well. Near field scanning optical microscopy is applied to map the Bloch states and bands.[29] Time resolution adds many possibilities to this technique.[30]

The effect of a PBG on the spontaneous emission of a source embedded in a PC may be observed both as an intensity inhibition[31] or as a change in the lifetime of the process.[32] In the latter case, both accelerated and slowed lifetime components can be observed. All these effects can be used to characterize the system.

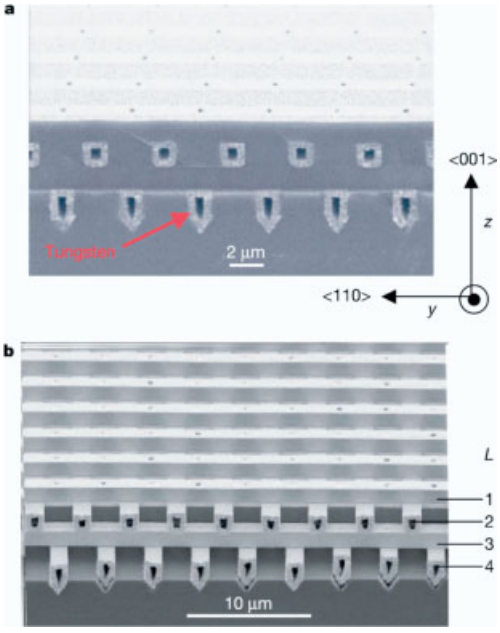

Fig. 7. Images of two stages of fabrication of a 3D tungsten PC. This metallic PBG structure has realized the channel of thermal emission into narrow discrete bands. Reprinted with permission, copyright 2002 Nature Publishing Group [34].

1.3. Applications

Current and foreseen applications of PCs can be divided according to their principle of functioning. Some rely on the existence or non-existence of a complete gap, others rely on the peculiar properties of the bands and their dispersion. Applications that rely on a gap make use of the suppressed DOS. Thus, the performance of solar cells or microelectronic devices can benefit from the suppression of spontaneous emission. Antennas for microwave applications may be made to emit only in the desired direction by placing them on a substrate with a PBG structure.[33] Some applications are entirely new and spring from the new physics brought about by PBG systems.

The spectrum of black-body radiation is very broad, which results in an important loss of efficiency when thermal sources are used for light generation: most of the energy is emitted as heat. A mechanism to prevent this might have been found in the use of metallic bandgap structures.[34] For 3D structures with the metal forming a continuous network (network topology) there is a cut-off frequency below which there are no propagating modes. If absorption can be neglected (thin structures) such an unusually large bandgap can be used to recycle IR blackbody radiation into the visible (VIS) spectrum. In the photon recycling process, an absolute 3D PBG completely frustrates IR thermal emission, and forces the radiation into a selective emission band. Energy is not wasted in heat generation, but channeled by a thermal equilibrium into useful emission at the edge of the bandgap. A prominent example is shown in Figure 7, where an all-metallic layer by layer structure is shown in two of the stages of its production. The tungsten 3D PC was made by selectively removing silicon from already fabricated polysilicon–SiO_2 structures, and refilling the resulting mold with tungsten by chemical vapor deposition (CVD).

A laser is basically a medium where population inversion is attained, whereby gain and amplification are achieved through stimulated emission. Spontaneous emission is the main foe to gain as it happens isotropically and cannot be prevented by (usually 1D) cavities. Cavities with a 3D complete gap present advantages in the sense that a single channel may be allowed for emission (through a defect with proper design) blocking other directions at the same time. Cavities in 2D systems are expected to present quality factors as high as tens of thousands and have been realized with several thousands.[35] Lasers have been realized in 2D and the race for lowering threshold is on.[36] Using one such cavity, laser action was demonstrated.[37] Two-level atoms cannot be made to lase in vacuum because the rate of stimulated emission equals absorption. Thus, at most, the population of the excited state reaches 1/2. Near a PBG edge, however, this situation changes, allowing for population inversion in two-level atoms. If a laser beam with intensity slightly below the threshold prepares such two-level atom system at a population near 1/2, a second low intensity beam may place the system in gain condition and constitute an all-optical transistor.[38]

There are a wealth of proposed applications relating to the guiding of light to make real circuits for communications and processing. In this class fall linear WGs, bendings, crossings, splittings, junctions, add-drop filters, etc., all necessary to direct the flow of light as electrons are directed by wires. WGs are routinely made in 2D systems by placing linear defects in

the desired configuration.[39] This is often done by removing rows of the elements constituting the PC. WGs can be made to bend through sharp corners with the enormous advantage in compaction as compared to ordinary fibers that can only be bent to a limited degree. The main workhorse in this field now is losses.[40] The optimization of guided mode properties and confinement in the third dimension, and the design of bends, systems to input and extract signals from the systems, etc., account for most of the effort spent in this research field. A WG can be bent on itself to form a ring that can be used as a laser cavity.[41] Modes in a WG may be designed to have linear dispersion and wide band width if many wavelengths are desired to be guided without pulse broadening—the RI is the same for every wavelength—or they can be designed to have nonlinear dispersion in order that different wavelengths feel different RIs, and thus reshaping of propagating pulses can be achieved. This may be very useful in optical communications. A WG consisting of a chain of coupled defects can act as a phase compensator if the right group velocity dispersion is designed.[42]

A 2D PC with a cavity in its center becomes a fiber when stretched in the third dimension.[43] Photons localize in the core and can only propagate in the axial direction. Such "holey" fibers rely on the existence of a 2D PBG held by cladding rather than on total internal reflection—the principle behind ordinary fibers. For that reason these fibers need not actually have a material core and can guide light through an air pipe, which makes them suitable for high power transmission: no undesirable nonlinear effects will be felt. On the other hand, if the core is made of a material properly doped with, for instance, a nonlinear material they can be made to amplify the signal, compress pulses, etc.

Systems with a complete PBG are difficult to fabricate but some useful properties still exist when no such gaps are available. Dispersion properties can be taken advantage of for steering light within a PC. Very anisotropic equi-energy surfaces are used for super-refraction, while the dispersive properties can be used for pulse reshaping.

Obviously a 1D PC (a Bragg reflector) cannot have a complete PBG: its gaps vary depending on direction such that a forbidden energy may be allowed to propagate just by changing the incidence angle. It can, however, be used as an omnidirectional reflector by placing the pseudogap within the light cone. Thus, even though there exist states of either polarization for any given energy (no gaps) there are certain ranges, for which the available states have $\boldsymbol{k}$s, which are inaccessible from outside the system.[44] These systems can be realized for any desired range and have a host of applications. The width of the omnidirectional reflection is mainly determined by the ratio of RIs of the layered materials and their ratio to the outer medium.[45] Using this principle hollow optical fibers are made where confinement of light in the hollow core is provided by the large PBG of an omnidirectional dielectric mirror.[46]

Proper design can allow for zero group velocity bands to contribute to laser action by enhancing the interaction between light and matter. Thus, a laser without a cavity can be realized[47] in which unit cell engineering can provide control of emission polarization.[48]

The laws of refraction take on surprising forms in PCs. Propagation being normal to the equi-energy surfaces, regions of high curvature produce very strong beam swings for slight changes in wavevector (superlens). Similarly in regions where curvature changes sign (inflexion points), ample changes in $\boldsymbol{k}$ produce negligible changes in propagation direction (supercollimation). Additional control can be gained with a sound choice of bands; thus, using electron-like bands (ω grows with $\boldsymbol{k}$—positive effective mass) yields a positive effective RI, whereas the use of hole-like bands (negative effective mass) allows for a negative effective RI.[49] Finally, in some regions of reciprocal space (usually where several Bragg planes meet) equi-energy bands show very strong energy dependence. The fact that a very slight change in energy results in a strong change of shape of the equi-energy surface can be applied to the design of a superprism.[50] The first demonstration is presented in Figure 8, where the deflection of two beams of very similar frequency is shown to behave very differently in a PC and in a homogeneous material. In 2D systems[51] this effect is being studied and experimentally implemented for multiplexers; more complex behavior has been described for self-assembled 3D systems.[52]

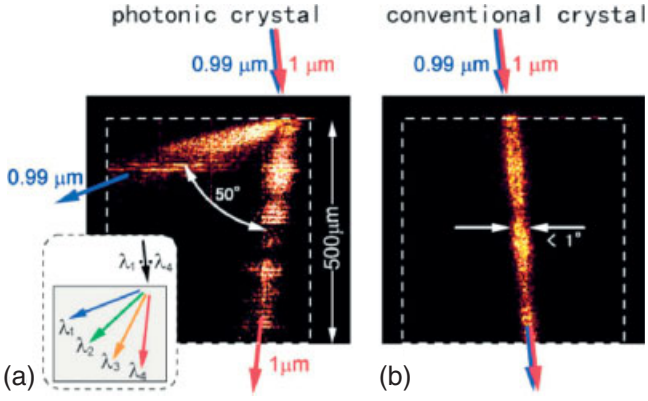

Fig. 8. At variance with a conventional crystal a PC can present a strong chromatic separation based on the superprism effect: beams of 0.99 μm and 1.0 μm suffer a very different refraction. Reprinted with permission, copyright 1999 American Institute of Physics [50].

1.4. Metamaterials

To close this section of introduction a few words on metamaterials should be said in order to better situate PCs in the materials world. Metamaterials is a general name for a larger class of materials whose properties (as represented by their electric permeability and magnetic permittivity) derive from their structure rather than from the materials composing them. PBG materials could be counted among them but the most striking examples are those with simultaneously negative ε and μ, called left-handed materials, where a negative RI is expected. Ordinary right-handed materials are such that $\boldsymbol{E}$, $\boldsymbol{H}$,

and $\boldsymbol{k}$ form a right-handed trihedron meaning that $\boldsymbol{E}\times\boldsymbol{H}\|\boldsymbol{k}$, so that the direction of propagation of energy coincides with that of the wavevector. For left-handed materials the opposite occurs $\boldsymbol{E}\times\boldsymbol{H}\|-\boldsymbol{k}$, and energy flows opposite to the wavevector. One crucial consequence is that negative refraction, as long ago described by Veselago,[53] may be realized,[54] relying on which perfect lenses can be designed.[55] So far, materials have been discussed in which the spectral position of optical features is close to the dimensions of their inner structure. In these ones, however, the periodicity of the structure occurs in a range much smaller than the wavelength, thus accounting for the use of effective ε and μ. Strong spectral dispersion is inherent in these peculiar metamaterials, where resonant phenomena involving some sort of plasma-like excitation are usually invoked. Applications for these materials are expected to enhance the performance of magnetic resonance imaging systems.[56] Other applications involve emission from sources embedded in metamaterials built as stacks of metallic grids immersed in foam.[57] It has been shown that directive emission from a source can be confined to a narrow cone based on the fact that an effective RI can be made to take on very small values. Thus every ray leaving the material forms a right angle irrespective of the angle it formed within the metamaterial.

Frequency selective surfaces[58] and PBG structures operate on the principle of resonance, based on multiple scattering by a series of periodically arranged metal or dielectric scatterers. Accordingly, the relevant frequencies, where their functions are closely related to the dimensions, define the periodicity. Fractals are mathematical objects with the unique property of being self-similar. This means that their general aspect is the same regardless of scale, that is, zooming in on the object's details gives a similar picture as zooming out for a panoramic view. This fact has a striking consequence on the resonances that can be sustained when such systems are built with scattering materials: the frequencies are detached from the scale. Such systems have been shown to present stop bands and pass bands like PCs over a broad range.[59] They can be built as 2D systems with design features well below the operating wavelength that can perform as 3D structures in terms of polarization- and incidence angle-independent reflection. Furthermore, the wavelengths of the lower gaps can be significantly longer than the size of the sample and can be driven by electrical signals.

Whether there can be PBGs without periodicity and without a BZ is a fundamental question. 1D superlattices stacked as Fibonacci series were shown to posses optical stop bands; similar phenomena were observed in acoustics, all of which fostered the search for PBGs in 2D quasiperiodic arrangements of dielectrics. These are structures arranged in orderly patterns that are not quite crystalline: the local symmetry is the same everywhere but there is no real overall periodicity. They are often built on forbidden rotational symmetries like 5-, 8-, or 12-fold. Sizeable gaps that do not depend on incidence direction are predicted for these 2D systems[60] and have been experimentally found in the long wavelength regime (10 GHz, where WGs can be produced)[61] and also in the far IR (100 μm).[62]

2. Preparation of PCs

A wave crystal can be designed for any interaction involving a wavy perturbation, be it light, sound, particles, spins, etc. It only entails designing the appropriate periodic structure, which, for EM interaction, is a PC. PCs may be built for any frequency range of the spectrum. Of course, the realization greatly changes according to the spectral range of functioning, principally owing to the size imposed by the wavelength. Therefore, the fabrication methods vary depending on the length scale. The first PC shown to have a complete PBG[63] was machined into a low loss dielectric material with millimeter size drills. The size determined its working range to be in the microwave regime. A scaling down of the process, it was suggested, would lead to similar systems working in the VIS spectrum. That challenge was actually faced and risen to,[64] but the method proved rather ineffective in the number of layers that could be produced. An entirely new structure was later proposed with a sizable, robust bandgap that could be built in a layer by layer fashion by stacking rods as a pile of logs.[65] This structure, initially realized in the GHz range, has been revealed as probably the best choice, and has been scaled down to optical frequencies by several means.

In what follows, a review of the methods employed to obtain systems functioning mainly in the optical range is presented, leaving the self-assembly techniques for a section of their own.

2.1. 1D Systems

1D systems have been produced and used widely for a long time as, for instance, antireflection coatings, notch filters, or distributed Bragg reflectors. Typically evaporation techniques were used. A few recent developments are described next with specific applications in photonics.

Although dendritic nanowires can hardly be classified as 1D structures, they can be described as a linear arrangement of light scatterers. These structures consist of grafted branches, periodically grown on a straight WG acting as a stem. The synthesis exploits the self-organized dendritic crystal growth to assemble microscale periodic semiconductor single crystal nanowires in a vapor transport and condensation system. Laser action was demonstrated using this structure as a resonator.[66]

Cholesteric liquid crystals (LC) present a layered structure in which in every layer molecules are aligned in parallel but rotated with respect to the layer underneath. They can be viewed as 1D PCs in which the dielectric anisotropy originates from the orientation of the molecular axes. The period is determined by the distance between the closest layers with parallel molecular axes, and the interaction with circularly polarized light gives rise to bands and gaps for transmission. Laser action can be sustained at the edges of the gap when such systems are properly doped with a dye.[67] The mode closest to the edge has the lowest lasing threshold.

ADVANCED MATERIALS

Layer by layer electrostatic assembly of polyelectrolytes is a technique that, combined with the in situ synthesis of inorganic nanoparticles, can lead to the formation of 1D structures with tuned morphologic (thickness) and dielectric properties (RI contrast).[68] These systems have potential as sensors since they respond to environmental changes in pH or ionic strength by swelling or shrinking, which changes their photonic signatures.

1D multilayers of controlled porosity can also be prepared by anodic etching of crystalline silicon.[69] The dielectric function is controlled through porosity, which, in turn, is controlled through current density in the electrochemical cell. The layer thickness is dictated by the etching time. These stacks can be designed to act as 1D Bragg reflectors. Cavities can be inserted where luminescent ions can be included by doping through cathodic electromigration of erbium into the porous silicon matrix, followed by high temperature oxidation. These structures can be used for biosensors after the inner surface of the porous Si is functionalized to bind some distinctive component in biological matter.[70]

2.2. 2D Systems

The fabrication of 2D PBG systems has experienced the greatest development, mainly boosted by the availability of mature techniques borrowed from many other areas. Lithography (mainly optical and electronic) is the main contributor to this explosive expansion since microelectronics had, for a long time, demanded more and more precise processing.

Carbon nanotubes with controllable diameters, from tens to hundreds of nanometers, and lengths of tens of micrometers can be grown on a large scale in a matter of minutes.[71] Plasma enhanced hot filament CVD is used with acetylene, serving as source of carbon, and often ammonia as a catalyst. The nanotubes grow on thin metal films or nanoparticles previously deposited by various means. Nanoparticles can eventually be arranged in an orderly way leading to ordered arrangements of long, parallel, straight, carbon nanotubes.[72] In such circumstances, the nanotubes act as scattering centers and produce a 2D PBG.

2D structure with a PBG in the near IR (NIR)[73] can be fabricated using a technology developed for the production of microchannel plates. This consists basically of drawing a bundle of optical fibers, in which core (SiO_2) and cladding (PbO) can be selectively dissolved. Thus the fibers are arranged in a hexagonal lattice and are drawn in order to reduce their diameter to the desired lattice parameter. The core is then dissolved, leaving behind a network of air holes in a glass matrix. The filling fraction of the air holes can be adjusted through the initial core/cladding radii ratio. The technique can be extended to produce nanochannels with optical features in the VIS and ultraviolet (UV).[74]

2D PBG structures have acquired the widest diffusion due to the easy, albeit expensive, implementation of microelectronic technology techniques, such as photolithography, electron beam lithography, etc. Monorails and air bridges are examples of 1D structures produced by these means.[75] Typically Si and III–V semiconductor technology is applied. Lattices composed of holes or pillars were often adopted to obtain different structures. The first such realization was in GaAs–GaAlAs,[76] where a lattice of holes was etched through an electron beam lithographed mask. WGs can be defined in these structures by leaving rows of holes undone. Point defects produced near such multiple wavelength carrying WGs can be tuned for extraction of selected wavelengths.[77] Figure 9 shows an example of a membrane PC where two defect holes near a WG with one row missing are tuned (by size) to extract selected wavelengths. Although these techniques are

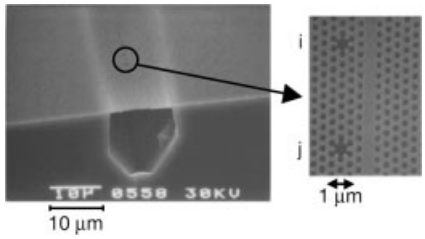

Fig. 9. EM picture of a straight waveguide in an InGaAsP 2D PC with isolated defects (labeled i and j) formed to couple to selected transmitted wavelengths. Reprinted with permission, copyright 2002 Nature Publishing Group [77].

mostly applied to produce 2D systems (where they are most effective), they can also be used in conjunction with other processes to add a third dimension to the structures obtained. By using relatively standard microelectronic techniques in a layer by layer fashion, 3D crystals were soon fabricated for the IR region.[78] As an alternative, wafer bonding[79] was used to build 3D structures where WGs can be easily integrated during production.[80]

Soft lithography, extensively reviewed by Xia and Whitesides,[81] is a non-photolithographic technique based on self-assembly and replica molding for micro- and nanofabrication. In soft lithography, an elastomeric stamp with patterned relief structures on its surface is used to generate patterns and structures with feature sizes ranging from 30 nm to 100 μm. Several techniques have been derived: micro-contact printing, replica molding, micro-transfer molding, micro-molding in capillaries, solvent-assisted micro-molding, etc. In nanoimprinting, a pattern recorded in a mold is press transferred to a thermoplastic polymer thin film, where ridges and trenches with a minimum size of 25 nm and a depth of 100 nm are created.[82] Further processing may be applied to record the transferred pattern into the substrate for large scale replication. Although a 2D technique, it can be extended for building 3D structures by iterative processing.

2D structures can be obtained in porous silicon when a lithographical mask is transferred by means of electrochemical pore formation.[83] The preservation of the shape of the pattern through hundreds of micrometers in depth is guaranteed by the fact that electrochemical etching proceeds only upon provision of optically created electronic holes that promote the Si dissolution at the tip of the pore. The factor con-

trolling the filling fraction is the illumination intensity. Therefore it can be used to shape the pores and confer on the structure a 3D character.[84]

2.3. 3D Systems

The border between 2D and 3D fabrication is sometimes rather diffuse because some 3D structures can be made with 2D techniques. Some can even range from 1D to 3D.

The transfer of corrugations from a patterned substrate can be made to act as an autocloning mechanism, through which a 3D structure can be grown by sequential deposition of Si and SiO_2.[85] The superprism effect was first demonstrated in these structures.[50] The technique initially developed for Si and SiO_2 was extended to new materials by direct growth[86] or by material exchange.[87]

AsSeTe chalcogenide glasses are materials that are photosensitive and have a large RI. These properties make these glasses particularly suitable for the fabrication of PCs. A grating is recorded in a thin layer of the chalcogenide by the interference of two laser beams. Since the material has a photoresist effect, it can be etched after exposure. The grooves are filled with a photoresist by spin coating and planarized. New material layers are evaporated on top and the process is repeated while rotating the orientation of the stripes. This technique is intrinsically self-aligned, providing a simple way to build layer-by-layer PCs.[88]

As seen above, two interfering beams produce a diffraction grating that can be used in interference lithography to record a grating; three beams produce a 2D pattern. To go one step further, a fourth beam adds depth to the structure to yield a 3D periodic lattice. The period of the structure and its symmetry (lattice) are dictated by the laser wavelength, the relative phases, and the incidence directions of the interfering beams, whereas the shape of the repeated feature in the lattice (basis) results from the beams' polarizations. This set-up applied to a photosensitive polymer can lead to a 3D network if the exposed polymer is crosslinked and the unexposed polymer is dissolved.[89] The resulting structure is depicted in Figure 10. Initially developed for pulsed-laser polymerization of UV-sensitive polymers, the technique has been extended to continuous-wave VIS lasers.[90] Exposed but undeveloped films are amenable to further processing by laser scanning to draw new structures for WG fabrication.[91] An unsatisfactory aspect of this technique is that the available photosensitive polymers (that have to be slightly absorbing to be sensitive but not in excess to allow exposure of the whole film) have low RIs. This makes a second process of templated infiltration necessary for the enhancement of the dielectric contrast. Recently, new materials[92] based on silica acrylate composites doped with transition metal oxides have proved to both comply with the need to be photosensitive and, thanks to the doping, permit an elevated RI above the threshold for a complete PBG in these structures. This template-free approach will allow the direct fabrication of 3D PCs where the RI can be controlled through the variation of the inorganic component of the sol–gel-derived photosensitive composites.

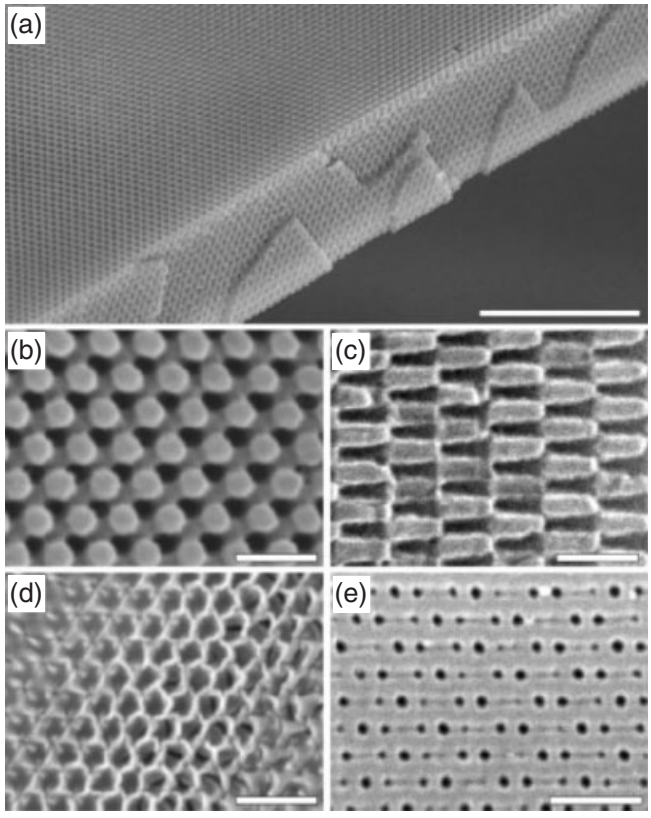

Fig. 10. SEM pictures of different structures obtained by the holography technique. Reprinted with permission, copyright 2002 Nature Publishing Group [89].

Deep X-ray lithography[93] allows an extra degree of precision and an extremely high depth of focus due to the reduced wavelength of the radiation used. A pattern is drawn on a resist and transferred to a metal sheet. This metal is then used as a mask, whose shade can be projected in different directions, tilted with respect to the normal, to produce rod structures. Simple methods may be used to replicate yablonovite structures in other materials.[94] The pattern can then be transferred to a metal (by electrodeposition) or a high RI dielectric (by a sol–gel technique).

Glancing-angle deposition[95] is a versatile technique that can be employed for the fabrication of large, 3D PBG crystals.[96] Physical vapor deposition with the vapor flux arriving at an oblique angle leads to the growth of inclined rods on the substrate. Rotation of the substrate by 90° every quarter period, changes the direction of the rod to form a square spiral. The vapor flux angle determines the pitch in the vertical direction. Tetragonal square spiral crystals with a predicted PBG can be produced in the visible, NIR, and IR spectrum. A tetragonal lattice suitable for a large PBG (up to 15 % for a silicon structure) can be synthesized by a regular array of square spiral structures grown from a simple, prepatterned substrate.[97]

Copolymers are formed by linking together two or more classes of monomers to form a larger molecule. In a block co-

ADVANCED MATERIALS

polymer, all of the monomers of each type are grouped together. A diblock copolymer can be thought of as two homopolymers joined together at the ends. Block copolymers self-assemble into 1D, 2D, and 3D periodic equilibrium structures with length scales in the 10–100 nm range. The plethora of structures into which block copolymers can be assembled, and the multiple degrees of freedom that they allow on the molecular level, offer a large parameter space for tailoring new types of PCs at optical length scales.[98] Very complex bicontinuous structures[99] with a 3D translation symmetry or composite systems with metallodielectric character are just two examples that can be realized with promising optical properties.

Layer-by-layer structures can be fabricated by 3D scanning of the focus of a pulsed laser in a resin film in order to draw the framework of a log pile structure by crosslinking the polymer. Femtosecond laser pulses are tightly focused inside the liquid resin, which is transparent to pulses below the two photon absorption threshold power density. The pulse intensity is adjusted so that the light power density at the focal spot of the laser beam exceeds the threshold. Strong absorption in this highly spatially localized region results in photopolymerization of the resin. By scanning the coordinates of the focal spot, predesigned patterns can be recorded in the liquid resin. Laser irradiation renders the exposed regions insoluble, while unexposed regions are dissolved in acetone and removed during the post processing stages.[100]

Similarly, focused ion beam micromachining can be used in conjunction with macroporous etching to produce replicas of the yablonovite structure.[101] A first set of holes is produced from a 2D mask by conventional photoassisted anodic dissolution. The focussed ion beam technique is then used to produce the other two set of holes. The structure thus produced is not exactly yablonovite, but a slightly distorted one.

Robot manipulation is a recently developed method that allows the arrangement of nano- and microscopic objects in 3D structures with a precision of nanometers and has allowed the first assembly of diamond opals.[102] The wood-pile structure that has been revealed as one of the best suited to sustain a complete PBG is amenable to construction by this method. This has recently been demonstrated by stacking previously fabricated grids.[103] The grids were defined by lithography as wires held by a frame and they were crisscross stacked to form a 3D crystal. Crystals for IR wavelengths of 3–4.5 μm of four to twenty layers (five periods), including one with a controlled defect, were integrated at predefined positions marked on a chip with an accuracy better than 50 nm. Microspheres are used to slot into holes defined in the frames to ensure correct alignment.

2.4. PC Fibers

A PC fiber, consisting of a pure silica core surrounded by a silica–air PC material with a hexagonal symmetry, was originally made by drawing a bundle of hollow silica rods, except for the center one that is solid. The drawing process thins the preform down to micrometer size, and fibers thus produced can support single robust low-loss guided modes over a very broad spectral range.[104] A fundamentally different type of optical WG structure is demonstrated, in which light is confined to the vicinity of a low RI region by a 2D PBG crystal.[105] The WG consists of an extra air hole in an otherwise regular honeycomb pattern of holes running down the length of the fiber. The core being air, guidance cannot occur through total internal reflection. Using the same principle but new materials, microstructured polymer optical fibers were also realized.[106] The low-cost manufacturability and the chemical flexibility of the polymers are here the main advantages.

A new concept in fiber fabrication was introduced by devising hollow fibers in which the wall is provided by an omnidirectional reflector.[46] These fibers comprise a hollow core surrounded by a multilayered cladding designed to reflect a certain range of frequencies that are guided.

3. Colloidal Crystals

Colloids are structures comprising small particles suspended in a liquid or a gas. In this context small refers to sizes between nanometers and micrometers, much larger than atoms or molecules but far too small to be visible to the naked eye. Sometimes these particles self-organize, owing to their electrostatic or other interactions, and give rise to crystalline structures. As such, they present the typical fingerprint of PCs: they are iridescent. Colloidal crystals can be used and studied as suspensions or can be further processed to obtain opals, which, in turn, can be used as templates for other materials. Colloids of spherical particles, reviewed by Xia et al.,[107] are more useful when ordered assembly is required because their interactions are more isotropic and stacking is easier. Next, an update of fine particles synthesis and assembly methods is provided along with some material aspects regarding infiltration and further processing.

3.1. Bare Opals

Opals are precious gems composed of sub-micrometer size silica spheres stacked together and cemented with a slightly different silica. This structure confers photonic properties[108] on the material and has inspired a whole branch of research in the PC field. Fine spherical particles have been produced from numerous materials, both inorganic (see review by Matijevic[109]) and organic such as polymers (see the comprehensive summary of synthesis and functionalization by Kawaguchi[110]), aiming at replicating the natural gems. This technique allows the widest range of materials and procedures of synthesis. Only the range of topologies is narrow since natural assembly tends to produce thermodynamically stable structures that are restricted to a few lattices, mostly compact cubic and

hexagonal. Furthermore, if special care is not taken, random stacking or disordered structures are obtained. This section is divided into two subsections reviewing particles synthesis and assembly, and further processing and fabrication.

3.1.1. Microsphere Synthesis and Assembly

As will be explained later on, the assembly of opals can be seen not only as a goal in itself but as a means for posterior templated synthesis of other materials. In this sense, the physicochemical properties of the material composing the initial opal must be taken into consideration. For this motive, silica has acquired a supremacy over other materials because it is highly inert both chemically and thermally. Thus, if infiltration requiring high temperature (a few hundred degrees Celsius) is envisaged, most organic polymers must be discarded in favor of silica.

The best known method for monodisperse silica spheres was originally developed by Stöber et al.[111] and relies on the hydrolysis of a silicon alkoxide and posterior condensation of alcohol and water to form siloxane groups. Because of their chemical structure, these beads present a surface charge that is screened by the ions in the medium. Under appropriate conditions of temperature, pH, and concentration this synthesis process yields spheres with diameters ranging from a few nanometers to a few micrometers. Although the reason why is still controversial, very monodisperse colloids (a few percent standard deviation in diameter) can be obtained for sizes between 200 and 600 nm. For larger sizes a strategy based on the growth in the presence of small seeds has proven successful.[112] Everything seems to indicate that the final size of the particles produced responds to a correct balance between the nucleation process (by which new particles are created) and that of aggregation (through which those particles grow at the expense of available monomers). For that reason, the concentration of seeds in a regrowth process must correctly match the reaction condition so that no nucleation occurs, while an optimum use of the silica precursor is made. Although most often the particles synthesized are spherical, ellipsoidal particles have also been produced by different methods such as ion irradiation[113] or inverse templating.[114]

Among the materials used for opal assembly the most widely spread are polymers; mainly polystyrene (PS) and poly(methyl methacrylate) (PMMA). For the preparation of these beads there are a host of techniques all under the umbrella of polymerization, but with different approaches such as precipitation polymerization, emulsion polymerization, dispersion polymerization, seeded polymerization, inversion emulsification, swelling polymerization, and suspension polymerization, and modifications of these that can be found in the review by Arshady.[115] Owing to a higher surface charge to density ratio, these particles tend to behave better than silica ones for the purpose of colloid crystallization. Therefore, they are very appropriate for optical and crystallization studies.

In order to obtain a PC, these beads must be arranged into a crystalline lattice. Depending on the properties of the particles used and the final product desired, various methods have been developed that are summarized next.

Some colloidal particles, owing to their mainly electrostatic interaction, tend to organize into crystalline lattices when the volume fraction reaches a certain value.[116] These crystals can be used for optical studies and find some applications, but their liquid character prevents some uses since they must be kept confined in vials or the like. The process of crystallization has been extensively studied and these structures serve as models for liquids and phase transition investigations. The interaction has for instance been studied in absence of gravity where only electrostatic forces intervene.[117] These systems reveal useful information for optical studies of the velocity of aggregation and make real space imaging possible.[118]

Fields other than gravity can be used to induce order in the colloidal systems. For instance an electric field can polarize the beads, which switches on a strong long-range interaction that quickly orders structures.[119] With AC fields, binary colloids present interesting behaviors depending on relative particles concentration and frequency.[120] Likewise, magnetic fields acting on colloids of magnetic beads (or non-magnetic beads immersed in magnetic liquids) produce ordered arrangements.[121] Crossed electric and magnetic fields can induce a martensitic-like transition from the body centered tetragonal (bct) to the fcc structure in mesocrystallites consisting of multiply coated spheres. The multiple coatings serve to enhance the electrorheologic and magnetorheologic effect.[122] EM fields have been used by producing (through interference) 3D standing waves in whose potential minima ions are trapped. They can similarly be used to trap dielectric spheres.[123] Fields can also be used, after crystallization is achieved, as a tool to remove defects from the crystal.[124] An annealing process provides the activation energy needed to relax existing defects without generating new ones. Optical tweezers use forces exerted by intensity gradients in strongly focussed laser beams to trap and move colloidal particles. Rapidly translating optical tweezers can be used to introduce elastic strain locally within a thin colloidal crystal, thereby delivering kinetic energy to the lattice without heating the surrounding fluid.

Sedimentation is the natural way to obtain solid opals. This method produces thick opals and can be altered in different ways depending on the goal pursued. In this procedure a colloid is left to settle, a process that takes between days and months depending on the size of the spheres, at the end of which a sediment is obtained.[125] The sedimentation occurs driven by gravity, and a clear sedimenting front can be seen in the vial separating clear water and colloid. When the concentration is low (~1 wt.-%) the beads behave as hard spheres and the velocity can be approximated by Stokes' law. As a matter of fact, this can be used to very accurately determine sphere size, if densities and viscosity are known. The supernatant liquid is removed and the sediment dried. At this stage the spheres are not in actual contact but kept together by water necks. The water content in the opal is about 10 wt.-% overall. A thermal treatment at 200 °C leaves the sample

water-free and makes it truly compact fcc, but, at the same time, makes it mechanically very weak and unmanageable. Additionally, drying in these conditions invariably involves a crack formation process that can barely be prevented when the lateral size of the sample is above tens of micrometers. Drying involves a contraction that does not occur in the supporting substrate, which can only be accommodated by the creation of cracks, as defects accommodate lattice mismatch in epitaxially grown materials. The final result is a compact of spheres arranged according to a fcc structure,[126] whose photonic properties scale with bead diameter revealing their origin.[127] A typical example is shown in Figure 11, where several facets are shown that belong to the fcc structure and are

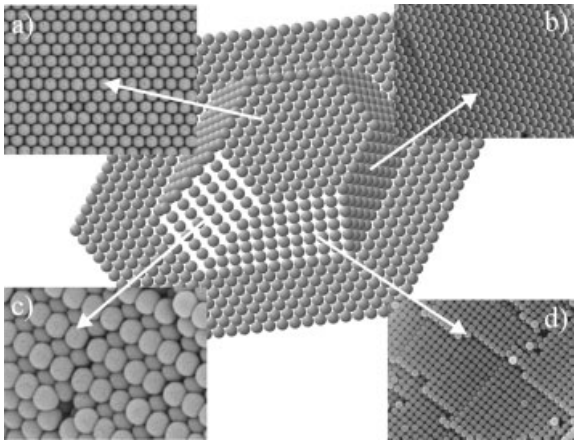

Fig. 11. Scanning electron microscopy (SEM) images of four facets in a real opal to be compared with a model crystal (center). a) Outer (111), b) inner (111), c) inner (110), and d) inner (100).

not found in other possible lattices like hexagonal close packed. The morphology includes the same kind of defects that can be expected in ordinary solids. This is manifested in optical spectra, mostly as a broadening of the peaks, diffuse scattering, and a decrease in reflectance (increase in transmission) at the gap frequency.[128] It is worth mentioning that for this kind of structure the best estimate for effective RI is the Maxwell–Garnett approximation[129] rather than a weighted average.

When beads are too large or too small (and so is their deposition velocity) bad quality or no sedimentation is achieved in a reasonable time; application of a vertical electric field on the sedimenting vessel can help in achieving sedimentation. This is rendered possible by the beads surface charge that makes them respond to a macroscopical electric field.[130] This way, large diameter beads can be slowed in their sedimentation, and small diameter spheres accelerated. The surface charge can be governed by pH, which gives one extra handle on the process. Limits on the highest voltage applicable are mainly imposed by medium electrolysis potential for the electrodes used.

The Langmuir–Blodgett method of thin film preparation used for organic materials can be adapted to the growth of thin film layers of fine particles.[131] Here, a single layer of monodisperse hydrophobic latex spheres or silica spheres rendered hydrophobic by the use of a suitable reagent can be spread at the air–water interface in a colloidal solution. If sufficient care is employed in the purification of the material such films can be compressed and deposited by the Langmuir–Blodgett technique to form ordered multilayers that show PBG properties. The compression causes the spheres to close pack on the water–air interface, which is required to create a close-packed layer on the substrate. The one layer process can be repeated several times to grow a 3D structure.[132] This method also allows a high degree of control in the synthesis of layered colloidal structures.

As opposed to the above mentioned method where a single layer is transferred to the substrate in each upstroke, polymer particles can be made to crystallize at the air–water interface by a combined effect of capillarity, aggregation, and thick film transfer to a substrate.[133] A beaker containing a colloidal suspension of spheres is heated and the particles near the water–air surface start protruding due to evaporation. The capillary forces make the floating spheres assemble and convection aggregates new particles from the bath to build new layers from underneath. The crystal thus formed can be transferred to a glass substrate introduced at an angle in the beaker.

The capillary forces present in an advancing (owing to evaporation) meniscus can be taken advantage of to assemble ordered layers of colloidal particles.[134] This was initially exploited for monolayer films and later extended to virtually any number of layers.[135] The method, very similar to Langmuir–Blodgett for film deposition, yields ordered arrays on nearly any vertical surface. The set up is simple and only requires a vial containing a colloid, where a flat substrate is inserted vertically. A meniscus is formed that draws particles to its vicinity by capillarity. Evaporation sweeps the meniscus along the substrate vertically, feeding particles to the growth front. Colloid concentration and sphere diameter determine the thickness of the layer deposited. Successive growth processes can lead to the assembly of multilayers that can be constituted of similar or different particles.[136] Although the evaporation rate can be easily controlled through the vapor pressure in the surrounding atmosphere, controlling the sedimentation rate is not so easy as it is largely determined by sphere size. A major challenge is encountered when the size of the particles is too large (larger than about 700 nm) so that the evaporation rate cannot match the sedimentation rate: very soon particles abandon the meniscus region and the entire mechanism fails. This problem was overcome by the application of a thermal gradient to the colloid.[137] The combination of Langmuir–Blodgett to grow a single layer of spheres with convective assembly to grow two confining thicker layers has facilitated the build up of embedded defect structures.[138]

Binary colloidal crystals can be grown in a layer-by-layer mode using a controlled drying process on vertical substrates.[139] A 2D hexagonal close-packed crystal of large (L) silica spheres is first grown on a clean glass substrate with a growth rate of 1 to 2 mm per day. The 2D crystal is then used

as a template, on which small (S) silica or PS particles are deposited. The small particles arrange themselves in regular structures depending on their volume fraction and size ratio. Another layer of large particles is deposited; these steps being successively repeated until a 3D structure of the desired thickness and composition is achieved. Structures with LS, LS_2, LS_3 formulas or kagomé lattices can be obtained depending on the size ratio and the concentration. If one of the two sizes is realized with latex, a non-compact structure can be obtained by calcination.

The method of growth in confinement cell[140] consists of the arrangement of particles from a colloid confined between two close flat surfaces. The confinement cell consists of two glass slides separated by a lithographically defined resist in the shape of a rectangular frame with draining channels, through which water leaks. One of the slides has a tube attached that serves to inject the colloid. The slides are kept together with binder clips. Sonication can be provided to help assembly. This ingenious method provides a route to grow thickness-controlled opals by varying the thickness of the spacer so that the desired number of layers can be selected just by spinning the appropriate amount of resist. Although this technique requires lithographic facilities, the spacer can be substituted for commercial mylar foil that serves the purpose equally well, although thicknesses are restricted to those foils available. Crystals formed simply by increasing the volume fraction beyond the liquid–solid phase transition tend to be small and predominantly randomly close packed. However, by forming these crystals while controlled shear to the glass plates bounding the crystal is applied, large-area single crystals can be made.[141] These crystals are much more regular and appear to be predominantly twinned fcc. The creation of single-orientational fcc crystals is possible when shear is applied in one direction.

In most of the methods described, a layer is assembled on or grows in contact with one confining wall. Through the interaction with the wall, this crystal facet tends to be the most compact possible and, as a consequence, the crystal naturally orients with the (111) planes parallel to the confining wall. It is sometimes desirable to obtain other orientations (for instance, to be able to do spectroscopy in other directions) or simply to extend the coherent growth length. To overcome this limitation, the use of patterned substrates has proven to be advantageous. For this purpose a substrate is designed with a pattern such that settling or arrangement of the colloid particles is directed and crystallization takes place according to a predefined geometry. This technique can be combined with others to attain thickness and orientation control at the same time. Ordinary sedimentation combined with a patterned substrate may lead to template-directed sedimentation,[142] which makes the growth in orientation other than the typical (111) possible. This colloidal epitaxy not only allows growth in exotic directions, but it also allows control over the size and shape of the grown crystal.

A system in which one of the slides of a confinement cell is properly patterned permits growth with control not only of thickness but also of orientation. This method relies on the dictation of structure and orientation by the pattern drawn on one of the confining walls. By means of ordinary or soft lithography a set of squares is recorded on a (100) silicon wafer that, through anisotropic etching, develops pyramidal pits. These pits can be designed such that their pitch is commensurate with the diameter of the spheres to be used. In this case, if growth initiates in the apex and proceeds to fill the pyramids, it can continue above the substrate to fill the whole confinement cell congruently.[143] By these means it has been possible to grow (100) oriented opals over areas as large as several square centimeters. This is not the only potential of the confinement cell with patterned floor, as various other structures can be grown, such as chiral chains with controlled handedness.[144] Clusters of a small number of beads in different arrangements can be assembled by adjusting the size and depth of the pits relative to the size of the spheres.[145]

A versatile method for the growth of vectorial structures that combines self-assembly, micro-fluidics, and soft lithography can be used to control thickness, area, orientation, and registry of silica colloidal crystals on silicon wafers.[146] This method relies on capillary forces to inject the suspension in V-grooves etched into a (100) Si wafer and on evaporation to assemble the spheres in a close-packed structure. For geometrical reasons the opaline structure grows with the (100) planes parallel to the (100) of the templating wafer. The number of layers is easily controlled through the depth of the V-grooves, which, in turn, is proportional to the etching time.

Normally vertical deposition is performed on plain flat substrates, but new possibilities emerge when the substrate is previously patterned in microchannels with vertical walls.[147] This can be done by anisotropic etching. In such cases, capillary forces at the surface relief drive the assembly of compact cubic structures, only in the concave trenches, with well oriented lattice planes. The use of these principles and vast possibilities offered by soft lithography allows the building of structures with varying thickness or lattice parameters in combination with all sorts of shapes and architectures.

When opals are grown on solid substrates drying leads to crack formation because contraction has to be accommodated by fissures. One ingenious way to circumvent this is to perform the growth on a liquid surface.[148] As the sample is not firmly attached to a solid, undeformable surface, shrinkage is allowed without the need for a tension relief by breach opening. Eligible liquids are, for instance, gallium and mercury, both with a high density. Using this method millimeter-wide crack-free samples can be produced.

It was mentioned earlier that one of the best, if not the best, structures for complete PBG formation is the diamond structure. This is an fcc with a two-atom basis that confers on the structure all the a priori required characteristics for bandgap opening. The lattice is as isotropic as it can be: the truncated octahedron that bounds its BZ is the closest to spherical of all possible. This implies that gaps opening at the boundaries of the BZ, whose energies are given by $\omega \sim ck_B/n$, will be very similar since all the boundaries of the BZ (k_B) are roughly the

same magnitude in all directions. The fact that the lattice presents a basis provides the extra ingredient: the lack of inversion symmetry that lifts degeneracies such as that at the W point.[10] In this structure the gap opens between the second and third bands and is relatively wide and robust. The dielectric contrast threshold for this structure is rather low ($\varepsilon_2/\varepsilon_1 \geq 2$), which makes it very enticing. Its assembly, however, from spherical beads has been elusive so far, and the structure has escaped researchers' hands and proved impossible. The reason is that the diamond lattice is very "empty", and colloidal methods tend to produce only compact structures. A method was proposed[149] to build the structure by using nanorobot-assisted manipulation that was soon after realized.[102] This method relies on the fact that two diamond lattices properly interpenetrated form a body-centered cubic (bcc) lattice. By building a mixed bcc lattice with two different materials, one of which is easily removable without affecting the other one, the goal can be realized. The nanorobot can place nano- to micrometric objects with nanometer precision, and plasma etching can remove latex without affecting silica. Direct growth (only one kind of spheres) was achieved too by making use of the contamination layer, inherent to the SEM observation, in order to glue particles together by their contact point. Thus, diamond lattices of silica spheres were obtained on silicon substrates, used as templates, where the first layer was held in place. A crystal is presented in Figure 12 as an example of (001) oriented direct growth.

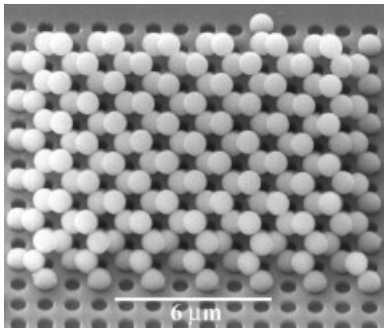

Fig. 12. A diamond lattice opal grown in the (100) direction by robot manipulation.

3.1.2. Further Processing

Once the opal is assembled various treatments can be applied that enhance its mechanical and other properties. Sintering, for instance, is a crucial treatment for thick freestanding opals for two reasons.

As-grown opals have a considerable amount of water, both physically and chemically bound, that can be removed by appropriate thermal treatment. This treatment is seen as essential if a close-packing filling fraction (ff) is to be achieved, since spheres in as-grown opals are not in close contact but separated by a thin water layer. The removal of water from the compact reduces the RI[150] and, as a consequence, blue shifts the Bragg wavelength. On the other hand, such thermal treatment may produce a matter viscous flow, through which spheres are bound together conferring mechanical strength on the opal. The latter process (called sintering and routinely used in ceramic processing) can be applied to control not only mechanical and chemical properties but also optical properties. There is, however, a more important effect associated with the flow of matter (that leads to the formation of necks between the spheres), which is the increase in filling fraction and the lattice parameter contraction. All this causes the optical features to blue shift by stages as the baking temperature is raised, first owing to the loss of water and finally to the contraction of the lattice.[151] This phenomenon, first observed in silica opals, was then seen to occur also in latex opals.[152] By changing the sintering temperature or time, the filling fraction can be controlled from close packing ($ff = 0.74$) to glass state ($ff = 1.0$), where no pores are left and photonic effects disappear.

In certain circumstances, control of the filling fraction or strengthening of the opal without altering the lattice parameter may be desired. Here an alternative method based on the growth of a thin silica,[153] or other oxide, layer by CVD is useful. Typically the reaction involved is the hydrolysis of a metal chloride to produce the metal oxide and hydrogen chloride. The water used is hydrogen bonded to the surface of the silica spheres, and can be recharged for further reactions by rehydrating through exposure to water vapor. This method allows the growth of several oxides by CVD at room temperature and atmospheric pressure, which have no adverse effects on the structure.

Apart from obtaining opals in desired forms by controlled growth, they can be used as a raw material for further processing in order to fabricate devices. In particular, they must be cut and polished. Although there has been little progress in this direction, some challenges are being explored.

When used in thin films, deposited opals may have to be lithographically or otherwise patterned. For instance, focused ion beams can be used to make trenches or vertical pits that can be used to connect different layers in a multiple stack. PMMA opals can be patterned through electron beam lithography[154] since this material is routinely used as a resist in microelectronic technology.

Recording a WG in the interior of an opal is a desirable goal if the opal can be made to sustain a PBG so that the WG could transmit light without loss. This could be done in steps by growing layers, some of which can be microlithographed. An ingenious way is to focus a writing beam on the interior of an opal whose pores are filled with a photopolymerizable resist.[91] By means of two-photon polymerization, a sharp boundary between exposed and unexposed resist can be achieved since this is a largely nonlinear process that occurs only in those regions very close to the focus, where intensity rises sharply to values high enough to produce the polymerization. Scanning the sample allows any desired shape to be drawn.

Silica opals can be carved by means of a microlapping machine in order to expose inner facets and to create micro-

prisms.[155] This can be done by attaching small pieces of opal at the end of a thinned glass drawn from a rod. A large single crystal domain has previously been marked by large current pulses of the electron microscope for optical identification. The opal, which can be rotated through different axes in order to properly orient it, is then polished with a microgrinder.

3.2. Composites

The mixing of different materials is used to provide structures with properties that a single component alone cannot offer. Thus, luminescence, magnetism, electrical conductivity, etc. are properties that a bare opal does not possess but can be supplied by the guest material. There are two main ways to make the composites: by synthesizing composite spheres prior to building the opal or by synthesizing new materials in or around the pores of an assembled opal. In either case, the mixed composition can be homogeneously distributed or shaped in shells in or around the spheres. Different approaches to produce each morphology have been explored and are explained next.

3.2.1. Composite-Particle Opals

Although core–shell beads are most often used, spheres with homogeneously distributed nanoparticle inclusions have also been synthesized. For instance, nanocomposite monodisperse silica spheres containing homogeneously dispersed silver quantum dots can be produced by the photochemical reduction of silver ions during hydrolysis of tetraethoxysilane in a microemulsion.[156] Depending on the timing, Ag quantum dots can be directed to different annuli within the silica spheres, as well as onto the silica sphere surface. Alternatively, inclusions, such as silicon, can be incorporated in the spheres by means of implantation techniques that confer new properties on the opals.[157]

Magnetically controllable PCs can be formed through the self-assembly of monodisperse magnetic colloidal spheres.[158] These contain nanoscale ferrite particles synthesized through emulsion polymerization. The diffraction from these PCs can be controlled through a magnetic field, which readily alters the PC lattice constant. Magnetic fields can also be used to strain the fcc lattice of superparamagnetic colloids polymerized within hydrogels or to control the PC orientation.

Particles of, mainly but not only, silica with an inner core or an outer or internal shell of other material may present many new properties that can find very important applications.[159] The commonest materials used can be classified into organic dyes, metals, and semiconductors.

Dyes, owing to their efficient luminescence, are often used to mark the spheres[160] by growing a thin internal shell. This opens a wide range of uses such as imaging the colloid formation[142] or studying defects in buried structures. They are also very useful in the study of the effects of a PBG on internal lucent sources. However, impregnation of an already assembled opal is much easier than dye coating at the sphere synthesis stage and more widely employed.

Metallodielectric systems have received much attention for their photonic interest and practical realizations have been tackled both from the metal-core or metal-cap particles and metal-infiltrated opal. The preparation and chemical reactivity of silver-core silica particles have been described;[161] similarly, gold colloids can be homogeneously coated with silica using a primer to render the gold surface vitreophilic.[162] After the formation of a thin silica layer in aqueous solution, the particles can be transferred into ethanol for further growth using the Stöber method. These spheres can finally be arranged into opal structures.[163] The opals thus built can be infiltrated with a polymer, and the silica can be subsequently dissolved. The result is an inverse polymer opal with the original metal cores confined in the holes left by the removed silica.[164] Conversely, metal shells can be grown on silica.[165] Reductive growth and coalescence of small gold nanoclusters attached to a functionalized surface leads to the formation of a closed gold layer. It is also possible to produce hollow gold shells by dissolution of the silica core and to coat the silica core gold shell particles with an additional outer silica shell. Layer by layer growth of polyelectrolyte combined with their exposure to suspensions of metal nanoparticles that bind themselves to the polyelectrolyte layers gives rise to organic spheres with dense shells of metallic nanoparticles.[166] Latex cores can be coated with magnetic shells, for instance, by adding ferrite nanoparticles polyelectrolyte layers to produce magnetic colloids.[167]

Nanometer-sized semiconductor particles such as CdS can be synthesized and subsequently surrounded by a homogeneous silica shell. The coating procedure uses a surface primer to deposit a thin silica shell in water, which can be grown so it becomes thicker in ethanol.[168] In a similar fashion CdTe, CdSe, and core–shell CdSe–CdS nanocrystals synthesized in aqueous solutions may be homogeneously incorporated as multiple cores into silica spheres of 40–80 nm size.[169] These can be grown into larger silica spheres by the Stöber technique, which gives semiconductor-doped silica globules of a desirable size in the submicrometer range.

3.2.2. Infiltrated Opals

Even though opals cannot exhibit a full PBG (regardless of the RI of the constituting spheres), the infiltration with materials of high enough RI may turn them into interesting structures, and more so when the underlying silica is removed: inverse opals (IO) can sustain a complete PBG. Infiltration with substances of RI higher than 2.8 times that of the opal spheres provides the structure with a full PBG.[170] Considering that silica has a RI of 1.45, this can rarely be achieved without removing the silica. This can be appreciated in Figure 13, where the gap width relative to the center position is plotted as a function of the infiltrated material RI for inverse fcc opals. Silicon, germanium, the III–Vs, and a few chalcogenides are the only materials complying with this requirement.

ADVANCED MATERIALS

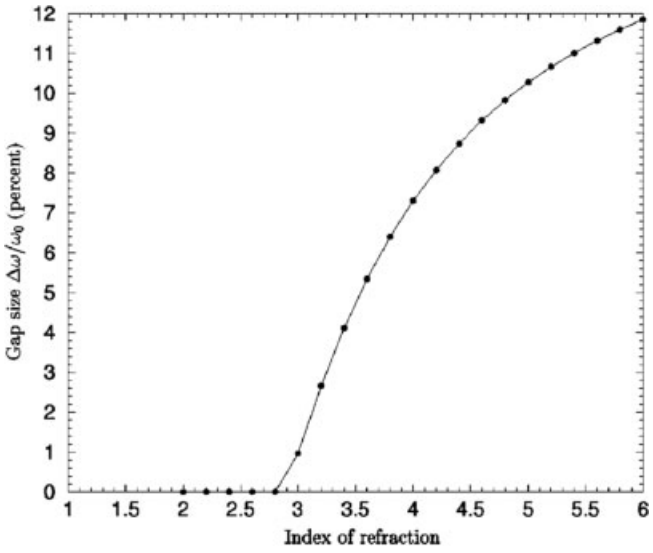

Fig 13. Gap width relative to the center position in percent for composite opals as a function of the RI ratio between background and spheres. The filing fraction is that of a compact fcc structure. Reprinted with permission, copyright 1998 American Physical Society [170].

There are, however, many interesting applications that do not require a complete PBG, such as sensors and super-refractive devices. IOs have even found applications as templates to grow spherical particles in their pore networks. When the goal is the build up of a complete PBG system the choice of material is not only determined by the RI but the electronic gap must also be taken into consideration. Of course, a high RI is required but the material must be transparent. As can be seen in Figure 14, the dielectric function decreases nearly exponentially with the electronic gap, making it hardly possible to find suitable materials transparent beyond 2.5 eV; that is, below 500 nm. Elemental materials are the easiest to synthesize but scarce. Compounds often require the reaction between two precursors, which is compromised by the special environment

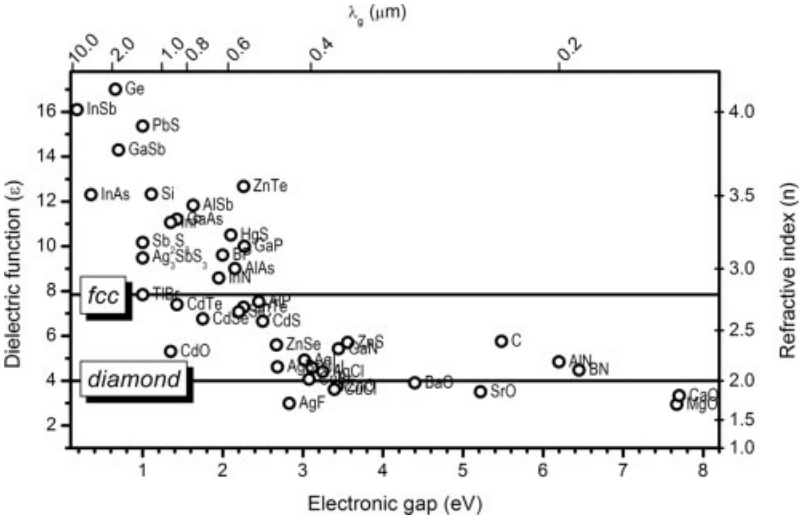

Fig. 14. Some materials dielectric and electronic coordinates. As can be seen, the greater the transparency range (larger electronic gap) the smaller the dielectric function. The threshold for complete PBG is indicated with horizontal lines for fcc and diamond opaline structures.

where reaction takes place not only in the way reactants are supplied but the ease with which products are eliminated. A good account of several periodic porous solids was given by Stein.[171] This section tries to contribute a summary of results regarding various materials of technological importance in photonics, along with the methods currently being used. Methods for the preparation of composites based on opals can be classified into three main categories. Wet methods are based on wet chemistry such as chemical bath deposition and electrodeposition, whereas dry methods are mainly based on reactions in the vapor phase. Injection of a molten substance (of low melting point) or infiltration with a suspension of nanoparticles can be classified as physical. One last consideration concerns the templating material itself. It must be kept in mind that certain reaction conditions, such as high temperature, may not be withstood by organic materials as polymers. This can restrict their use as compared to silica—much more chemically inert and thermally stable.

In the classification of compounds a division according to the electronic properties can be convenient.

Polymers can be easily synthesized within the pore network of opals just by impregnating with the monomer and then polymerizing it; inversion by dissolution of the original matrix leads to a perfect polymer replica.[172] Conducting polymers have a great interest and can be synthesized in the preformed opals by electro-[173] or other polymerization, and can show electrical conductivity and luminescent properties.[174] If the eletropolymerization is performed on a thick sedimented opal, the thickness of the final infiltrated opal can be controlled by the reaction time.[175] Since polymerization occurs from the working electrode (substrate) and proceeds upwards, increasing numbers of layers from the opal get cemented by the growing polymer. The reaction is stopped at any desired moment and excess layers (not bound by the polymer) can be washed away. The original spheres can then be removed by dissolution. Polymers can be used for two-step templating in a "lost wax" mode, whereby a replica from an opal (an IO) is used to template a second generation opal of nearly any desired material.[114] In this way it is possible to generate a wide variety of highly monodisperse inorganic, polymeric, and metallic solid and core–shell colloids, as well as hollow colloids with controllable shell thickness.

Hydrogels usually consist of randomly cross-linked polymer chains and contain a large amount of water filling interstitial spaces of the network, resulting in amorphous structures. Colloidal PS spheres can be easily made to crystallize, and if in their presence a hydrogel is polymerized that can be functionalized with a molecular recognition element to sense a given chemical agent, a specific sensor is created. In particular, certain metal ions can be made to covalently attach to the hydrogel PC through complexes that cross-link the hydrogel and

make it contract, blue-shifting its spectral features.[176] The same principle can be used to sense carbohydrates,[177] redox state,[178] pH, or ionic strength.[179] Hydrogel-encapsulated colloidal crystals can also find applications as mechanochromic PCs.[180] Upon removal of water and reswelling, a completely water-free robust composite can be made. Glass transition temperature tunability (through monomer(s) composition) is granted that allows for a wide range of optical–mechanical properties.

LCs are a set of materials with tunable RI: their molecules are largely anisotropic so that their polarizability depends on the orientation of the molecules. The change of orientation varies the RI and, as a result, when included in a periodic dielectric the photonic band structure changes. They were shown to change the band structure of opal upon infiltration, but, more interestingly, they could be used to enable thermal tuning of the optical properties.[181] By controlling the temperature around the phase transition, an abrupt change in RI can be attained. Thermal tuning is slow and electric control is more desirable. Based on the RI change caused by molecular reorientation in an electric field, a stop band can be driven by the field produced between the electrodes confining a thin opal film.[182] If an inverse, rather than a direct opal, is filled with a LC a higher volume fraction is obtained, which gives greater control over the optical properties.[183] In this case an abrupt change in the stop band is demonstrated. One further step can be made by infiltrating an IO with a photochromic azo dye in the LC. Illumination can induce the photochemical isomerization of the azo LC molecules from a rod-like shape into a bent one. This transition destabilizes the phase structure and randomizes the dielectric function distribution changing the band structure.[184] The most remarkable feature is that the isomerization is reversible by shining UV light on the structure, which makes this a light-driven switch.

Organic dyes have long been known for their efficient emission and used mostly as laser media. They are usually dissolved in organic solvents that facilitate impregnation and can be mixed with polymerizable compounds. All these properties have made them a perfect playground to probe the effects of PBGs on emitters embedded in PCs. Inhibition and stimulated emission were first observed in rhodamine dissolved in a polymer IO.[185] The effects of the PBG can also be observed in the luminescence lifetime.[32] The stop band in these structures does not constitute a complete PBG and, as a consequence, shifts with angle with the corresponding effect on luminescence.[186] However, when the dielectric contrast is very strong the gaps widen and the angular dispersion may be negligible.[31] These structures may be made to lase[187] even in the absence of a complete PBG through a gap-enhanced distributed feed back process. Lasing can occur in different directions depending on the interplay between the dye emission band and the pseudogap.[188] Laser emission can even be obtained simultaneously in various directions if two dyes are infiltrated in the same piece of opal and properly pumped.

Dyes infiltrated in opals have served to demonstrate that intragap propagation is possible through excitations created by a highly polarizable medium with resonant frequency coupled to the PC.[189] These excitations are formed due to interaction between the (opal) Bragg gap and the (dye) polariton gap. As a result the Bragg reflectivity plateau splits into two peaks, with a transmission spectral region in between. A similar effect was observed when an organic–inorganic layered perovskite[190] is introduced in the opal matrix such that the exciton couples to the opal stop band demonstrating a Rabi splitting.

The tuning or control of the photonic response with light is a major technological goal for whose realization several routes have been followed. A molecular aggregate is a collection of molecules in which the individual molecules are closely coupled and respond in-phase to an external EM field. Collective coherent response in the molecular aggregate contributes a giant oscillation. Apparently, the giant oscillation can induce dramatic changes in the RI around the resonant frequency. Thus, a photochromic dye aggregate in which the resonance frequency of the aggregated state is close to the PBG, while that of the non-aggregated state is far from the gap, would enable one to induce a large change in the stop band by illumination. Phototunable PBG crystals constituted from photochromic dyes and silica spheres have been fabricated by evaporating dye into the voids of opals. The dye undergoes photoisomerization upon illumination with UV light. The RI change induced by aggregate formation is quite large compared to the change induced by an orientation change of LC molecules or by the photochromic effect at the single-molecule level. The induction of such large changes of RIs provides a new approach toward the synthesis of materials with both large and small RIs.[191] The crystallization of a colloid depends on the balance of electrostatic forces between spheres. These forces can be strongly screened by free ions in the solution. Thus, dye molecules such as malachite green[192] that can be photoionized may permit a control on crystal order–disorder phase transitions induced by UV light irradiation.

Ferroelectric materials other than LCs have been synthesized within opals, owing to the enormous increase in dielectric constant expected at the phase transition (divergent for materials with a second order transition). Thus, a giant enhancement of the dielectric constant (up to $\sim 10^8$ at 100 Hz) in sodium nitrite infiltrated opals was found.[193] Barium,[194] strontium, and lead titanate[195] in silica opals were also sol–gel synthesized with modest effects on the photonic properties. The same is true for barium titanate IOs.[196] This, however, is not surprising, since divergence occurs only for static (or very low frequency) dielectric constant but not for the optical limit. Lithium niobate ($LiNbO_3$) is one of the most interesting materials for electro-optic and photorefractive applications.[197] $LiNbO_3$ IOs can be prepared using polyelectrolyte multilayer coated PS opals as templates for a sol–gel process and removing the initial opal by calcination.

Insulators have been explored in order to extend their use from other fields, where they have long standing applications, to opening areas in photonics. For instance, interesting behavior should be obtainable for carbon-based structures with a dimensional scale between fullerenes or nanotubes and graphit-

ADVANCED MATERIALS

ic microfibers. Thus, CVD produced carbon IOs provide examples of both dielectric and metallic optical PCs.[198] Most metal oxides, due to their insulator character, present a fairly low and non-dispersive RI. They have been synthesized in the opal, mainly by electrochemical deposition or by hydrolysis of alkoxides. For instance, zinc oxide,[199] tungsten trioxide,[200] and lead oxide[201] were obtained by electrochemical deposition, and tin oxide by hydrolysis.[202] Among them, titanium dioxide has the highest dielectric constant. Its RI is not enough, however, to open a full PBG in the IO. More so considering that the phase resulting from the synthesis is the lower RI one: anatase. The high RI phase, rutile, may be obtained by thermal annealing of anatase, but this process severely disrupts the structure. Nevertheless, its ease of preparation (hydrolysis of titanium alkoxide, chloride, or other precursors) and the range of studies it allows has made it very popular. When a diluted alkoxide is employed in several cycles, shell structures grow around the templating spheres.[203] As an alternative, the use of highly concentrated alkoxides in a slow, one-cycle process where a gel is initially formed in the pores, leads, upon calcination, to a titania skeleton structure.[204] This novel structure has very interesting properties as is the build up of two complete PBGs as opposed to common IOs where only one PBG occurring between the eighth and ninth bands is found. Physical methods have also been developed based on a dipping process, whereby co-assembly of monodisperse polystyrene spheres and nanoparticles of silica and titania from aqueous suspension is followed by a calcination treatment. It is possible to continuously adjust the position of the stop band of the IO by controlling the nanoparticle volume fractions.[205] Recently a method was described through which nanoparticles in the rutile phase were synthesized at room temperature from titanium tetrachloride.[206] These particles were infiltrated in the latex opal by centrifugation, and the template was removed by calcination without affecting the titania crystallographic phase.

Most materials introduced in opals as light sources have broad luminescence bands that cannot be completely blocked by the opal stop band. On the contrary, rare earth ions present narrow bands that may overcome this concern. These ions can be obtained from their salts (like europium from its nitrate) to outwardly impregnate assembled opals,[207] or can be integrated in the opal spheres adding rare earth salt (like erbium from its chloride) at the time of synthesis.[208] Alternatively, fluorescent erbium-doped titania nanoparticles can be synthesized through a sol–gel process followed by peptization and hydrothermal treatment[209] that can, subsequently, be used to infiltrate previously assembled opals.

Magnetic materials have been introduced in opals not only but mostly for the magneto-optical properties they develop in this periodic environment.[210] By proper spatial arrangement of magnetic and dielectric components it should be possible to construct magnetic PCs with strong spectral non-reciprocity: $\omega(\boldsymbol{k}) \neq \omega(-\boldsymbol{k})$. This spectral asymmetry, in turn, results in a number of interesting phenomena; in particular, one-way transparency: the magnetic PC, being transparent for a wave of frequency ω, becomes opaque for the same frequency propagating in the opposite direction. The practical realizations comprise magnetic nanoparticles, precipitation from aqueous ferrofluid to form composite (then inverse) opals,[211] synthesis of polyferrocenysilane for magnetic ceramic IO,[212] or even ferromagnetic perovskite manganite, a colossal magnetoresistance material.[213] Potential applications for such a magnetoresistive ferromagnetic material are diverse, including a field tunable optical switch. A Faraday rotator has been fabricated in the form of a colloidal suspension with dysprosium nitrate dissolved.[214] An enhancement of the rotation is found in the stop band region due to multiple scattering.

The very interesting properties that arise when metals are involved (often associated with plasmons and a negative dielectric function) results in them being of high technological interest. Originally, infiltration of opals with metals such as gold was attained by filtration through a smooth membrane with pores that retained the latex and the gold particles but allowed flux of water.[215] Another physical method is the assembly of latex microspheres in the presence of concentrated gold nanoparticles. Thick multilayer latex crystals grew upon drying the films, probably due to the combination of the increasing latex volume fraction and convective assembly.[216] Periodic nanosphere arrays can be fabricated by a sequential templated infiltration. First a carbon IO is produced where molten metals are infiltrated at close to the melting point and pressures of 1–2 kbar, resulting in nanosphere crystals for elemental metals and semiconductors (Pb, Bi, Sb, and Te) and thermoelectric alloys (Bi-Sb, Bi-Te, and Bi-Te-Se).[217]

Thiol surface-functionalized silica opals immersed in a toluene solution containing gold nanocrystals (that affix to the colloidal surfaces at the thiol sites) are partially covered with gold. These templates are then immersed in electroless deposition baths, and metal formation in the pores readily occurs.[218]

Electrochemical deposition from a metal chloride in a typical three-electrode set up is, by far, the most widely used method. To grow gold in opals, the sample (assembled on an indium tin oxide, ITO, substrate) is masked (to confine growth to the sample region), suspended in the electrolyte solution with the Pt counter electrode, and a potentiostatical deposition is performed.[219] Nickel and gold electrodeposition can also be performed (on opals copper sputtered on the back) galvanostatically resulting in a dark opalescent metal 100 μm thick membrane.[220] Platinum, palladium, and cobalt IOs are also prepared by electrochemical deposition on polystyrene latex spheres self-assembled on gold electrodes in a matter of minutes. In this case, the thickness of the metal film is controlled through the charge passed. The polystyrene spheres are fully removed by washing in toluene.[221] Metal IOs can be used for sequential templating. In the first step an opal slab is electrochemically infiltrated with nickel. After removal of the opal template the nickel mesh is slowly oxidized. The resulting poorly conducting nickel oxide mesh is then used as a nanomold for the electrochemical growth of a gold nanosphere array. Finally, the nickel oxide template is removed in dilute sulfuric acid to produce an array of gold nanospheres.[217]

Mechanical processing of pre-formed 3D metal IOs has lead to lower dimensional structures.[222] 1D PCs (corrugated nanowires), and 2D metal-mesh PCs of between one and fifty sheets may be made by this process. Possible applications that could be enabled include fibrous PC colorants for plastics and 1D PC wires.

Semiconductors have been introduced in opal structures owing to their optical and electronic properties. The reduced electronic bandgap makes them interesting for electronic and opto-electronic applications, but, at the same time implies (recall the correlation in Fig. 14) an elevated RI, which makes them good candidates for PBG applications. Very different synthesis methods have been used to produce composites and IOs depending on their elemental or compound nature.[223] Different application have been proposed depending on their opto-electronic characteristics.

Silicon is a very interesting material with current microelectronics technology in mind. It would be desirable to develop PCs that could be directly integratable with the current technology. Additionally, its RI is well beyond the threshold for complete PBG opening in IO configuration, and it is transparent in the communications window (ca. 1.5 μm). Considering that opal templating competes favorably with most other methods of PC fabrication, as far as cost, ease, and large scale production are concerned, it is not surprising that this has been one of the first systems where a complete PBG has been realized in the optical spectrum. The first silicon IO was synthesized by CVD in silica opaline matrices obtained by sedimentation in ethylene glycol aqueous solution.[224] The precursor used was disilane, which decomposes at elevated temperature (ca. 300 °C), but not so elevated that the underlying opal could not withstand it. The reaction produces an amorphous silicon shell around the spheres and, if desired, it can be crystallized by thermal annealing. A typical example is shown in Figure 15 where thin silicon shells can be seen after dissolving the underlying silica from the templating opal. Sintering of the initial opal provides the connectivity required for the etchant to be able to dissolve the silica when inverting the structure. The opal was designed in order that the complete PBG of the final structure fell into the optical communication wavelength. Following this approach, but using a different method for the assembly of the opal, thin film IOs were produced.[225] Similarly IO fibers were produced by growing silicon within opals assembled in confined environments, such as microchannels, where the opals are assembled with well controlled orientation.[226] The existence of a complete PBG in these systems was further supported by measuring the reflectivity in the principal directions of propagation.[227] It was found that a frequency band existed common to all of the propagation directions where transmission is prevented.

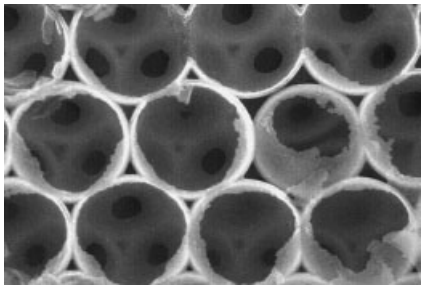

Fig. 15. SEM image of a silicon IO with a very low filing fraction.

The material with the highest RI in the optical spectrum is germanium. Its absorption edge is however small, which restricts its use at wavelengths greater than about 1.8 μm. This, in turn, sets the periodicity of the opals where useful structures can be built to large values, so that the spheres in a complying fcc lattice must be larger than 1.1 μm in diameter. Although germanium can be synthesized through a two step process of hydrolysis of an alkoxide (to form GeO_2) and reduction to metallic Ge; this procedure yields granular material and is laborious.[228] At variance, the CVD method grows layer by layer high-quality material and is quicker and simpler.[229] The precursor can be germane, which has a convenient decomposition temperature (270 °C), and the infiltration can be controlled by the precursor pressure or baking time and temperature. Electrodeposition has also proven to work for this synthesis. Germanium tetrachloride is used, and amorphous Ge is obtained that can be crystallized by thermal annealing.[230] Layered Si–Ge structures can be grown by CVD in opals. The control of semiconductor shell thickness and sequence, along with the selective oxidation, as well as the ability to etch the oxides opens a vast range of possibilities in PBG engineering. Thus, structures with mixed layers of silicon, germanium, both oxides, and air can be easily and precisely created where double complete PBGs can be hosted.[231]

III–V semiconductors have extremely interesting opto-electronic properties. They have luminescence, large dielectric functions and nonlinear coefficients, and a mature technological backup. They are commonly grown by molecular beam epitaxy or CVD, but their synthesis is difficult in the opal environment. This is the case because two molecules are involved and the reaction must happen in a very intricate network of interstices; single source precursors have not achieved much success. Indium phosphide[232] and gallium phosphide[233] have been produced by atmospheric pressure metal organic CVD. Electrochemical deposition is the only method that has succeeded in the synthesis of gallium arsenide in opals.[234] The depositions of III–V semiconductor films on silica opals was much more difficult to achieve than those of II–VIs mainly because of the more covalent (less ionic) character of the former.

Gallium nitride has become a very interesting material due to its wide bandgap and thermal stability. Its introduction in opals has been realized by direct synthesis from metal gallium or its oxide (liquid at room temperature) annealed in the presence of nitrogen hydrides.[235]

Selenium IOs can be prepared by imbibing a direct silica opal with molten selenium under pressure. Pressure is required because selenium does not wet silica.[236] Chalcogenides, such as cadmium sulphide[237] or selenide,[238] were first

physically infiltrated in opals by soaking the porous structures with suspensions of quantum dots that presented optical gain near the PC stop band edge.[239] Evaporation of the solvent results in precipitation and formation of the composite. Subsequently, the template is removed and a 3D patterned material consisting solely of densely packed nanocrystals is obtained. The nanocrystals can be sintered (nanocrystals melt at temperatures much lower than the bulk) to form a macroporous bulk semiconductor. Chemical bath deposition methods, where two precursors supply the ions in successive impregnations, can be used to control the degree of infiltration, allowing the production of cadmium sulfide[240] or antimony sulfide (Sb_2S_3) inverse opals.[241] However, electrochemical synthesis produces better quality material both of CdS and CdSe.[242] Furthermore, the method has proved itself versatile enough to produce virtually any selenide, telluride, or sulfide. Only detailed studies of deposition parameters (current density, deposition time, concentrations of electrolytes, solvents, and temperatures) must be carried out first.[234] Gas–solid reaction techniques, where a gas is passed through a pretreated opal, have facilitated the synthesis of tin sulphide[243] and lately antimony sulphide, the only semiconductor with silicon and germanium for which a complete PBG has been obtained.[244] The latter is a very interesting material with one of the highest RI available (enough to open a complete PBG) and a broad electronic gap. Under these conditions, a complete PBG has been demonstrated in the visible region, which might set a record as the highest energy gap in opal based structures.

4. Summary

The field of PCs is in continuous expansion (more than a thousand papers can be counted this half year alone) and a review ages swiftly. I have tried to give a comprehensive overview of the state of the art with emphasis in the use of colloidal systems for photonics applications. Many groups in the world are carrying out research in this field in different EM ranges, with different aims, and employing different approaches. The use of self-assembly techniques for the optical range is very widespread, and materials science knowledge and techniques are used extensively. New materials are being explored every day, and old materials are being found useful for emerging needs. Classification has become very difficult because metals, semiconductors, and insulators can be found among organic, inorganic, and hybrid materials that present themselves in multiple forms, phases, and flavors, and can be viewed differently according to which of their properties they are chosen for. The bottom line is that new ways will emerge in which research will profit from very different sources of knowledge.

Some profound questions remain unanswered, such as will the ultimate PBG device be all-optical or will it be electronic + optical? Most probably the answer will be the latter because the boundaries of the device will themselves be diffuse. More so if we consider the very likely integration in the bio and molecular worlds, towards which the field will inevitably drift. This will surely provide new questions for those that think that there is no new science left to unveil, only development. There is also the question whether 2D will be enough or 3D will be needed. It is undeniable that, if complete photon confinement is required for some application, 2D techniques will surely be insufficient. 3D systems other than self-assembled structures entail rather expensive production strategies, and cost is a very strong constraint. Almost certainly we shall see the merging of techniques coming from the 2D and microelectronics background and techniques from self-assembly.

Received: June 6, 2003
Final version: August 4, 2003

[1] E. Yablonovitch, *Phys. Rev. Lett.* **1987**, *58*, 2059.
[2] S. John, *Phys. Rev. Lett.* **1987**, *58*, 2486.
[3] H. E. Hinton, D. F. Gibbs, *J. Insect. Physiol.* **1969**, *15*, 959.
[4] J. V. Sanders, *Nature* **1964**, *204*, 1151.
[5] For example, see C. Kittel, *Introduction to Solid State Physics*, 3rd ed., John Wiley, New York **1968**.
[6] I. I. Tarhan, G. H. Watson, *Phys. Rev. B* **1996**, *54*, 7593.
[7] K. W. K. Shung, Y. C. Tsai, *Phys. Rev. B* **1993**, *48*, 11 265.
[8] M. I. Antonoyiannakis, J. B. Pendry, *Europhys. Lett.* **1997**, *40*, 613.
[9] a) K. M. Leung, Y. F. Liu, *Phys. Rev. Lett.* **1990**, *65*, 2646. b) Z. Zhang, S. Satpathy, *Phys. Rev. Lett.* **1990**, *65*, 2650.
[10] K. M. Ho, C. T. Chan, C. M. Soukoulis, *Phys. Rev. Lett.* **1990**, *65*, 3152.
[11] J. D. Joannopoulos, R. D. Meade, J. N. Winn, *Photonic Crystals: molding the flow of light*, Princeton University Press, Princeton, NJ **1995**.
[12] This can be otherwise viewed as a statement of a variational principle. The lowest energy eigenvalue is always orthogonal to all those of smaller energy and minimizes the energy functional $E_f = 1/2 \langle \boldsymbol{H}(\boldsymbol{r}) | \Theta | \boldsymbol{H}(\boldsymbol{r}) \rangle / \langle \boldsymbol{H}(\boldsymbol{r}).\boldsymbol{H}(\boldsymbol{r}) \rangle$.
[13] S. Datta, C. T. Chan, K. M. Ho, C. M. Soukoulis, *Phys. Rev. B* **1992**, *46*, 10 650.
[14] K. Sakoda, *Optical Properties of Photonic Crystals*, Springer Series in Optical Sciences, Vol. 80, Springer, Berlin **2001**.
[15] It is worth noting that the point X ((001) direction) does not show such a gap at the edge of the BZ, which is in agreement with a simple prediction based on structure factor from X-ray scattering. However, if the dielectric contrast is strongly increased a small gap opens signaling the failure of that theoretical approach.
[16] H. S. Sözüer, J. W. Haus, R. Inguva, *Phys. Rev. B* **1993**, *45*, 13 962.
[17] N. W. Ashcroft, N. D. Mermin, *Solid State Physics*, Rinehart & Wilson, Philadelphia, PA **1976**.
[18] Fluctuations of the EM field may induce the emission from an excited atom and the transfer of its energy into the EM field. The opposite is not possible since fluctuations cannot excite a ground state atom if there is no energy in the field.
[19] S. John, J. Wang, *Phys. Rev. Lett.* **1990**, *64*, 2418.
[20] W. L. Vos, M. Megens, C. M. van Kats, P. Bosecke, *Langmuir* **1997**, *13*, 6004.
[21] W. M. Robertson, G. Arjavalingam, R. D. Meade, K. D. Brommer, A. M. Rappe, J. D. Joannopoulos, *Phys. Rev. Lett.* **1992**, *68*, 2023.
[22] A. Imhof, W. L. Vos, R. Sprik, A. Lagendijk, *Phys. Rev. Lett.* **1999**, *83*, 2942.
[23] W. L. Vos, H. M. van Driel, *Phys. Lett. A* **2000**, *272*, 101.
[24] A remarkable feature of this gap is that its position is determined by very linear dispersion bands; as a consequence, its position can be well approximated by an effective RI. This fact permits the use of the Snell law to determine the wavevector inside the PC and the mapping of the bands.
[25] A. Talneau, L. Le Gouezigou, N. Bouadma, *Opt. Lett.* **2001**, *26*, 1259.
[26] D. Labilloy, H. Benisty, C. Weisbuch, T. F. Krauss, R. Houdre, U. Oesterle, *Appl. Phys. Lett.* **1997**, *71*, 738.
[27] V. N. Astratov, D. M. Whittaker, I. S. Culshaw, R. M. Stevenson, M. S. Skolnick, T. F. Krauss, R. M. De La Rue, *Phys. Rev. B* **1999**, *60*, R16 255.
[28] T. Kanai, T. Sawada, K. Kitamura, *Langmuir* **2003**, *19*, 1984.
[29] P. L. Phillips, J. C. Knight, B. J. Mangan, P. S. J. Russell, M. D. B. Charlton, G. J. Parker, *J. Appl. Phys.* **1999**, *85*, 6337.
[30] M. L. M. Balistreri, H. Gersen, J. P. Korterik, L. Kuipers, N. F. van Hulst, *Science* **2001**, *294*, 1080.

[31] A. F. Koenderink, L. Bechger, H. P. Schriemer, A. Lagendijk, W. L. Vos, *Phys. Rev. Lett.* **2002**, *88*, 143 903.
[32] E. P. Petrov, V. N. Bogomolov, I. I. Kalosha, S. V. Gaponenko, *Phys. Rev. Lett.* **1998**, *81*, 77.
[33] E. R. Brown, C. D. Parker, E. Yablonovitch, *J. Opt. Soc. Am. B* **1993**, *10*, 404.
[34] J. G. Fleming, S. Y. Lin, I. El-Kady, R. Biswas, K. M. Ho, *Nature* **2002**, *417*, 52.
[35] J. Vuckovic, M. Loncar, H. Mabuchi, A. Scherer, *Phys. Rev. E* **2002**, *6501*, 016 608.
[36] M. Loncar, T. Yoshie, A. Scherer, P. Gogna, Y. M. Qiu, *Appl. Phys. Lett.* **2002**, *81*, 2680.
[37] O. Painter, R. K. Lee, A. Scherer, A. Yariv, J. D. O'Brien, P. D. Dapkus, I. Kim, *Science* **1999**, *284*, 1819.
[38] S. John, K. Busch, *J. Lightwave Technol.* **1999**, *17*, 1931.
[39] S.-Y. Lin, E. Chow, V. Hietala, P. R. Villeneuve, J. D. Joannopoulos, *Science* **1998**, *282*, 274.
[40] H. Benisty, D. Labilloy, C. Weisbuch, C. J. M. Smith, T. F. Krauss, D. Cassagne, A. Beraud, C. Jouanin, *Appl. Phys. Lett.* **2000**, *76*, 532.
[41] S. H. Kim, H. Y. Ryu, H. G. Park, G. H. Kim, Y. S. Choi, Y. H. Lee, J. S. Kim, *Appl. Phys. Lett.* **2002**, *81*, 2499.
[42] K. Hosomi, T. Katsuyama, *IEEE J. Quantum Electron.* **2002**, *38*, 825.
[43] P. Russell, *Science* **2003**, *299*, 358.
[44] J. N. Winn, Y. Fink, S. H. Fan, J. D. Joannopoulos, *Opt. Lett.* **1998**, *23*, 1573.
[45] Y. Fink, J. N. Winn, S. H. Fan, C. P. Chen, J. Michel, J. D. Joannopoulos, E. L. Thomas, *Science* **1998**, *282*, 1679.
[46] B. Temelkuran, S. D. Hart, G. Benoit, J. D. Joannopoulos, Y. Fink, *Nature* **2002**, *420*, 650.
[47] M. Meier, A. Mekis, A. Dodabalapur, A. Timko, R. E. Slusher, J. D. Joannopoulos, O. Nalamasu, *Appl. Phys. Lett.* **1999**, *74*, 7.
[48] S. Noda, M. Yokoyama, M. Imada, A. Chutinan, M. Mochizuki, *Science* **2001**, *293*, 1123.
[49] M. Notomi, *Phys. Rev. B* **2000**, *62*, 10 696.
[50] H. Kosaka, T. Kawashima, A. Tomita, M. Notomi, T. Tamamura, T. Sato, S. Kawakami, *Appl. Phys. Lett.* **1999**, *74*, 1370.
[51] L. J. Wu, M. Mazilu, T. Karle, T. F. Krauss, *IEEE J. Quantum Electron.* **2002**, *38*, 915.
[52] T. Ochiai, J. Sanchez-Dehesa, *Phys. Rev. B* **2001**, *64*, 245 113.
[53] V. G. Veselago, *Sov. Phys. Usp.* **1968**, *10*, 509.
[54] R. A. Shelby, D. R. Smith, S. Schultz, *Science* **2001**, *292*, 77.
[55] J. B. Pendry, *Phys. Rev. Lett.* **2000**, *85*, 3966.
[56] M. C. K. Wiltshire, J. B. Pendry, I. R. Young, D. J. Larkman, D. J. Gilderdale, J. V. Hajnal, *Science* **2001**, *291*, 849.
[57] S. Enoch, G. Tayeb, P. Sabouroux, N. Guerin, P. Vincent, *Phys. Rev. Lett.* **2002**, *89*, 213 902.
[58] B. A. Munk, *Frequency Selective Surfaces, Theory and Design*, Wiley, New York **2000**.
[59] W. J. Wen, L. Zhou, J. S. Li, W. K. Ge, C. T. Chan, P. Sheng, *Phys. Rev. Lett.* **2002**, *89*, 223 901.
[60] Y. S. Chan, C. T. Chan, Z. Y. Liu, *Phys. Rev. Lett.* **1998**, *80*, 956.
[61] C. J. Jin, B. Y. Cheng, B. Y. Man, Z. L. Li, D. Z. Zhang, S. Z. Ban, B. Sun, *Appl. Phys. Lett.* **1999**, *75*, 1848.
[62] M. Hase, H. Miyazaki, M. Egashira, N. Shinya, K. M. Kojima, S. Uchida, *Phys. Rev. B* **2002**, *66*, 214 205.
[63] E. Yablonovitch, T. J. Gmitter, K. M. Leung, *Phys. Rev. Lett.* **1991**, *67*, 2295.
[64] C. C. Cheng, A. Scherer, *J. Vac. Sci. Technol. B* **1995**, *13*, 2696.
[65] K. M. Ho, C. T. Chan, C. M. Soukoulis, R. Biswas, M. Sigalas, *Solid State Commun.* **1994**, *89*, 413.
[66] H. Yan, R. He, J. Johnson, M. Law, R. J. Saykally, P. Yang, *J. Am. Chem. Soc.* **2003**, *125*, 4728.
[67] V. I. Kopp, B. Fan, H. K. M. Vithana, A. Z. Genack, *Opt. Lett.* **1998**, *23*, 1707.
[68] T. C. Wang, R. E. Cohen, M. F. Rubner, *Adv. Mater.* **2002**, *14*, 1534.
[69] H. A. Lopez, P. M. Fauchet, *Appl. Phys. Lett.* **2000**, *77*, 3704.
[70] S. Chan, S. R. Horner, P. M. Fauchet, B. L. Miller, *J. Am. Chem. Soc.* **2001**, *123*, 11 797.
[71] Z. F. Ren, Z. P. Huang, J. W. Xu, J. H. Wang, P. Bush, M. P. Siegal, P. N. Provencio, *Science* **1998**, *282*, 1105.
[72] K. Kempa, B. Kimball, J. Rybczynski, Z. P. Huang, P. F. Wu, D. Steeves, M. Sennett, M. Giersig, D. Rao, D. L. Carnahan, D. Z. Wang, J. Y. Lao, W. Z. Li, Z. F. Ren, *Nano Lett.* **2003**, *3*, 13.
[73] K. Inoue, M. Wada, K. Sakoda, A. Yamanaka, M. Hayashi, J. W. Haus, *Jpn. J. Appl. Phys., Part 2* **1994**, *33*, L1463.
[74] A. Rosenberg, R. J. Tonucci, E. A. Bolden, *Appl. Phys. Lett.* **1996**, *69*, 2638.
[75] K. Y. Lim, D. J. Ripin, G. S. Petrich, L. A. Kolodziejski, E. P. Ippen, M. Mondol, H. I. Smith, P. R. Villeneuve, S. Fan, J. D. Joannopoulos, *J. Vac. Sci. Technol. B* **1999**, *17*, 1171.
[76] J. R. Wendt, G. A. Vawter, P. L. Gourley, T. M. Brennan, B. E. Hammons, *J. Vac. Sci. Technol. B* **1993**, *11*, 2637.
[77] S. Noda, A. Chutinan, M. Imada, *Nature* **2000**, *407*, 608.
[78] S. Y. Lin, J. G. Fleming, D. L. Hetherington, B. K. Smith, R. Biswas, K. M. Ho, M. M. Sigalas, W. Zubrzycki, S. R. Kurtz, J. Bur, *Nature* **1998**, *394*, 251.
[79] S. Noda, N. Yamamoto, A. Sasaki, *Jpn. J. Appl. Phys., Part 2* **1996**, *35*, L909.
[80] S. Noda, K. Tomoda, N. Yamamoto, A. Chutinan, *Science* **2000**, *289*, 604.
[81] Y. N. Xia, G. M. Whitesides, *Annu. Rev. Mater. Sci.* **1998**, *28*, 153.
[82] S. Y. Chou, P. R. Krauss, P. J. Renstrom, *Science* **1996**, *272*, 85.
[83] U. Gruning, V. Lehmann, C. M. Engelhardt, *Appl. Phys. Lett.* **1995**, *66*, 3254.
[84] F. Müller, A. Birner, J. Schilling, U. Gösele, C. Kettner, P. Hänggi, *Phys. Status Solidi A* **2000**, *182*, 585.
[85] S. Kawakami, T. Kawashima, T. Sato, *Appl. Phys. Lett.* **1999**, *74*, 463.
[86] T. Sato, K. Miura, N. Ishino, Y. Ohtera, T. Tamamura, S. Kawakami, *Opt. Quantum Electron.* **2002**, *34*, 63.
[87] O. Hanaizumi, M. Saito, Y. Ohtera, S. Kawakami, S. Yano, Y. Segawa, E. Kuramochi, T. Tammura, S. Oku, A. Ozawa, *Opt. Quantum Electron.* **2002**, *34*, 71.
[88] A. Feigel, Z. Kotler, B. Sfez, A. Arsh, M. Klebanov, V. Lyubin, *Appl. Phys. Lett.* **2000**, *77*, 3221.
[89] M. Campbell, D. N. Sharp, M. T. Harrison, R. G. Denning, A. J. Turberfield, *Nature* **2000**, *404*, 53.
[90] S. Yang, M. Megens, J. Aizenberg, P. Wiltzius, P. M. Chaikin, W. B. Russel, *Chem. Mater.* **2002**, *14*, 2831.
[91] W. M. Lee, S. A. Pruzinsky, P. V. Braun, *Adv. Mater.* **2002**, *14*, 271.
[92] K. Saravanamuttu, C. F. Blanford, D. N. Sharp, E. R. Dedman, A. J. Turberfield, R. G. Denning, *Chem. Mater.* **2003**, *15*, 2301.
[93] G. Feiertag, W. Ehrfeld, H. Freimuth, H. Kolle, H. Lehr, M. Schmidt, M. M. Sigalas, C. M. Soukolis, G. Kiriakidis, T. Pedersen, J. Kuhl, W. Koenig, *Appl. Phys. Lett.* **1997**, *71*, 1441.
[94] C. Cuisin, A. Chelnokov, D. Decanini, D. Peyrade, Y. Chen, J. M. Lourtioz, *Opt. Quantum Electron.* **2002**, *34*, 13.
[95] K. Robbie, M. J. Brett, *J. Vac. Sci. Technol. A* **1997**, *15*, 1460.
[96] S. R. Kennedy, M. J. Brett, O. Toader, S. John, *Nano Lett.* **2002**, *2*, 59.
[97] O. Toader, S. John, *Science* **2001**, *292*, 1133.
[98] Y. Fink, A. M. Urbas, M. G. Bawendi, J. D. Joannopoulos, E. L. Thomas, *J. Lightwave Technol.* **1999**, *17*, 1963.
[99] A. M. Urbas, M. Maldovan, P. DeRege, E. L. Thomas, *Adv. Mater.* **2002**, *14*, 1850.
[100] H. B. Sun, S. Matsuo, H. Misawa, *Appl. Phys. Lett.* **1999**, *74*, 786.
[101] A. Chelnokov, K. Wang, S. Rowson, P. Garoche, J. M. Lourtioz, *Appl. Phys. Lett.* **2000**, *77*, 2943.
[102] F. Garcia-Santamaria, H. T. Miyazaki, A. Urquia, M. Ibisate, M. Belmonte, N. Shinya, F. Meseguer, C. Lopez, *Adv. Mater.* **2002**, *14*, 1144.
[103] K. Aoki, H. T. Miyazaki, H. Hirayama, K. Inoshita, T. Baba, K. Sakoda, N. Shinya, Y. Aoyagi, *Nat. Mater.* **2003**, *2*, 117.
[104] J. C. Knight, T. A. Birks, P. S. Russell, D. M. Atkin, *Opt. Lett.* **1996**, *21*, 1547.
[105] J. C. Knight, J. Broeng, T. A. Birks, P. S. J. Russel, *Science* **1998**, *282*, 1476.
[106] M. A. van Eijkelenborg, M. C. J. Large, A. Argyros, J. Zagari, S. Manos, N. A. Issa, I. Bassett, S. Fleming, R. C. McPhedran, C. M. de Sterke, N. A. P. Nicorovici, *Opt. Express* **2001**, *9*, 319.
[107] Y. N. Xia, B. Gates, Y. D. Yin, Y. Lu, *Adv. Mater.* **2000**, *12*, 693.
[108] J. V. Sanders, *Nature* **1964**, *204*, 1151.
[109] E. Matijevic, *Chem. Mater.* **1993**, *5*, 412.
[110] H. Kawaguchi, *Prog. Polym. Sci.* **2000**, *25*, 1171.
[111] W. Stöber, A. Fink, E. Bohn, *J. Colloid Interface Sci.* **1968**, *26*, 62.
[112] G. H. Bogush, M. A. Tracy, C. F. Zukoski, *J. Non-Cryst. Solids* **1988**, *104*, 95.
[113] E. Snoeks, A. van Blaaderen, T. van Dillen, C. M. van Kats, M. L. Brongersma, A. Polman, *Adv. Mater.* **2000**, *12*, 1511.
[114] P. Jiang, J. F. Bertone, V. L. Colvin, *Science* **2001**, *291*, 453.
[115] R. Arshady, *Colloid Polym. Sci.* **1992**, *270*, 717.
[116] P. N. Pusey, W. van Megen, *Nature* **1986**, *320*, 340.
[117] J. X. Zhu, M. Li, R. Rogers, W. Meyer, R. H. Ottewill, W. B. Russell, P. M. Chaikin, *Nature* **1997**, *387*, 883.
[118] U. Gasser, E. R. Weeks, A. Schofield, P. N. Pusey, D. A. Weitz, *Science* **2001**, *292*, 258.
[119] M. Trau, D. A. Saville, I. A. Aksay, *Science* **1996**, *272*, 706.
[120] W. D. Ristenpart, I. A. Aksay, D. A. Saville, *Phys. Rev. Lett.* **2003**, *90*, 128 303.

[121] A. T. Skjeltorp, *Phys. Rev. Lett.* **1983**, *51*, 2306.
[122] P. Sheng, W. Wen, N. Wang, H. Ma, Z. Lin, W. Y. Zhang, X. Y. Lei, Z. L. Wang, D. G. Zheng, W. Y. Tam, C. T. Chan, *Pure Appl. Chem.* **2000** *72*, 309.
[123] M. M. Burns, J. M. Fournier, J. A. Golovchenko, *Science* **1990**, *249*, 749.
[124] P. T. Korda, D. G. Grier, *J. Chem. Phys.* **2001**, *114*, 7570.
[125] R. Mayoral, J. Requena, J. S. Moya, C. Lopez, A. Cintas, H. Miguez, F. Meseguer, L. Vazquez, M. Holgado, A. Blanco, *Adv. Mater.* **1997**, *9*, 257.
[126] H. Miguez, F. Meseguer, C. Lopez, A. Mifsud, J. S. Moya, L. Vazquez, *Langmuir* **1997**, *13*, 6009.
[127] H. Miguez, C. Lopez, F. Meseguer, A. Blanco, L. Vazquez, R. Mayoral, M. Ocaña, V. Fornes, A. Mifsud, *Appl. Phys. Lett.* **1997**, *71*, 1148.
[128] V. N. Astratov, A. M. Adawi, S. Fricker, M. S. Skolnick, D. M. Whittaker, P. N. Pusey, *Phys. Rev. B* **2002**, *66*, 165 215.
[129] S. Datta, C. T. Chan, K. M. Ho, C. M. Soukoulis, *Phys. Rev. B* **1993**, *48*, 14 936.
[130] M. Holgado, F. Garcia-Santamaria, A. Blanco, M. Ibisate, A. Cintas, H. Miguez, C. J. Serna, C. Molpeceres, J. Requena, A. Mifsud, F. Meseguer, C. Lopez, *Langmuir* **1999**, *15*, 4701.
[131] K. U. Fulda, B. Tieke, *Adv. Mater.* **1994**, *6*, 288.
[132] M. Bardosova, P. Hodge, L. Pach, M. E. Pemble, V. Smatko, R. H. Tredgold, D. Whitehead, *Thin Solid Films* **2003**, *437*, 276
[133] S. H. Im, Y. T. Lim, D. J. Suh, O. O. Park, *Adv. Mater.* **2002**, *14*, 1367.
[134] N. D. Denkov, O. D. Velev, P. A. Kralchevsky, I. B. Ivanov, H. Yoshimura, K. Nagayama, *Langmuir* **1992**, *8*, 3183.
[135] P. Jiang, J. F. Bertone, K. S. Hwang, V. L. Colvin, *Chem. Mater.* **1999**, *11*, 2132.
[136] P. Jiang, G. N. Ostojic, R. Narat, D. M. Mittleman, V. L. Colvin, *Adv. Mater.* **2001**, *13*, 389.
[137] Y. A. Vlasov, X. Z. Bo, J. C. Sturm, D. J. Norris, *Nature* **2001**, *414*, 289.
[138] K. Wostyn, Y. Zhao. G. Schaetzen, L. Hellemans, N. Matsuda, K. Clays, A. Persoons, *Langmuir* **2003**, *19*, 4465.
[139] K. P. Velikov, C. G. Christova, R. P. A. Dullens, A. van Blaaderen, *Science* **2002**, *296*, 106.
[140] S. H. Park, D. Qin, Y. Xia, *Adv. Mater.* **1998**, *10*, 1028.
[141] R. M. Amos, J. G. Rarity, P. R. Tapster, T. J. Shepherd, S. C. Kitson, *Phys. Rev. E* **2000**, *61*, 2929.
[142] A. van Blaaderen, R. Ruel, P. Wiltzius, *Nature* **1997**, *385*, 321.
[143] Y. D. Yin, Y. N. Xia, *Adv. Mater.* **2002**, *14*, 605.
[144] Y. D. Yin, Y. N. Xia, *J. Am. Chem. Soc.* **2003**, *125*, 2048.
[145] Y. D. Yin, Y. N. Xia, *Adv. Mater.* **2001**, *13*, 267.
[146] S. M. Yang, G. A. Ozin, *Chem. Commun.* **2000**, 2507.
[147] S. M. Yang, H. Miguez, G. A. Ozin, *Adv. Funct. Mater.* **2002**, *12*, 425.
[148] B. Griesebock, M. Egen, R. Zentel, *Chem. Mater.* **2002**, *14*, 4023.
[149] F. Garcia-Santamaria, C. Lopez, F. Meseguer, F. Lopez-Tejeira, J. Sanchez-Dehesa, H. T. Miyazaki, *Appl. Phys. Lett.* **2001**, *79*, 2309.
[150] F. Garcia-Santamaria, H. Miguez, M. Ibisate, F. Meseguer, C. Lopez, *Langmuir* **2002**, *18*, 1942.
[151] H. Miguez, F. Meseguer, C. Lopez, A. Blanco, J. S. Moya, J. Requena, A. Mifsud, V. Fornes, *Adv. Mater.* **1998**, *10*, 480.
[152] B. Gates, S. H. Park, Y. N. Xia, *Adv. Mater.* **2000**, *12*, 653.
[153] H. Míguez, N. Tétreault, B. Hatton, S. M. Yang, D. Perovic, G. A. Ozin, *Chem. Commun.* **2002**, *2377*, 2736.
[154] M. Muller, R. Zentel, T. Maka, S. G. Romanov, C. M. S. Torres, *Chem. Mater.* **2000**, *12*, 2508.
[155] R. Fenollosa, M. Ibisate, S. Rubio, C. Lopez, F. Meseguer, J. Sanchez-Dehesa, *J. Appl. Phys.* **2003**, *93*, 671.
[156] W. Wang, S. A. Asher, *J. Am. Chem. Soc.* **2001**, *123*, 12 528.
[157] J. Valenta, J. Linnros, R. Juhasz, J. L. Rehspringer, F. Huber, C. Hirlimann, S. Cheylan, R. G. Ellman, *J. Appl. Phys.* **2003**, *93*, 4471.
[158] X. L. Xu, G. Friedman, K. D. Humfeld, S. A. Majetich, S. A. Asher, *Adv. Mater.* **2001**, *13*, 1681.
[159] F. Caruso, *Adv. Mater.* **2001**, *13*, 11.
[160] A. Vanblaaderen, A. Vrij, *Langmuir* **1992**, *8*, 2921.
[161] T. Ung, L. M. Liz-Marzan, P. Mulvaney, *Langmuir* **1998**, *14*, 3740.
[162] L. M. Liz-Marzan, M. Giersig, P. Mulvaney, *Langmuir* **1996**, *12*, 4329.
[163] F. Garcia-Santamaria, V. Salgueirino-Maceira, C. Lopez, L. M. Liz-Marzan, *Langmuir* **2002**, *18*, 4519.
[164] B. Rodriguez-Gonzalez, V. Salgueirino-Maceira, F. Garcia-Santamaria, L. M. Liz-Marzan, *Nano Lett.* **2002**, *2*, 471.
[165] C. Graf, A. van Blaaderen, *Langmuir* **2002**, *18*, 524.
[166] Z. J. Liang, A. S. Susha, F. Caruso, *Adv. Mater.* **2002**, *14*, 1160.
[167] F. Caruso, A. S. Susha, M. Giersig, H. Mohwald, *Adv. Mater.* **1999**, *11*, 950.
[168] M. A. Correa-Duarte, M. Giersig, L. M. Liz-Marzan, *Chem. Phys. Lett.* **1998**, *286*, 497.
[169] A. L. Rogach, D. Nagesha, J. W. Ostrander, M. Giersig, N. A. Kotov, *Chem. Mater.* **2000**, *12*, 2676.
[170] K. Busch, S. John, *Phys. Rev. E* **1998**, *58*, 3896.
[171] A. Stein, *Microporous Mesoporous Mater.* **2001**, *44*, 227.
[172] H. Miguez, F. Meseguer, C. Lopez, F. Lopez-Tejeira, J. Sanchez-Dehesa, *Adv. Mater.* **2001**, *13*, 393.
[173] K. Yoshino, S. Satoh, Y. Shimoda, Y. Kawagishi, K. Nakayama, M. Ozaki, *Jpn. J. Appl. Phys., Part 2* **1999**, *38*, L961.
[174] M. Deutsch, Y. A. Vlasov, D. J. Norris, *Adv. Mater.* **2000**, *12*, 1176.
[175] T. Cassagneau, F. Caruso, *Adv. Mater.* **2002**, *14*, 34.
[176] S. A. Asher, A. C. Sharma, A. V. Goponenko, M. M. Ward, *Anal. Chem.* **2003**, *75*, 1676.
[177] S. A. Asher, V. L. Alexeev, A. V. Goponenko, A. C. Sharma, I. K. Lednev, C. S. Wilcox, D. N. Finegold, *J. Am. Chem. Soc.* **2003**, *125*, 3322.
[178] A. C. Arsenault, H. Miguez, V. Kitaev, G. A. Ozin, I. Manners, *Adv. Mater.* **2003**, *15*, 503.
[179] K. Lee, S. A. Asher, *J. Am. Chem. Soc.* **2000**, *122*, 9534.
[180] S. H. Foulger, P. Jiang, A. Lattam, D. W. Smith, J. Ballato, D. E. Dausch, S. Grego, B. R. Stoner, *Adv. Mater.* **2003**, *15*, 685.
[181] K. Yoshino, Y. Shimoda, Y. Kawagishi, K. Nakayama, M. Ozaki, *Appl. Phys. Lett.* **1999**, *75*, 932.
[182] Y. Shimoda, M. Ozaki, K. Yoshino, *Appl. Phys. Lett.* **2001**, *79*, 3627.
[183] M. Ozaki, Y. Shimoda, M. Kasano, K. Yoshino, *Adv. Mater.* **2002**, *14*, 514.
[184] S. Kubo, Z. Z. Gu, K. Takahashi, Y. Ohko, O. Sato, A. Fujishima, *J. Am. Chem. Soc.* **2002**, *124*, 10 950.
[185] K. Yoshino, S. B. Lee, S. Tatsuhara, Y. Kawagishi, M. Ozaki, A. A. Zakhidov, *Appl. Phys. Lett.* **1998**, *73*, 3506.
[186] S. G. Romanov, T. Maka, C. M. S. Torres, M. Muller, R. Zentel, *Appl. Phys. Lett.* **1999**, *75*, 1057.
[187] S. V. Frolov, Z. V. Vardeny, A. A. Zakhidov, R. H. Baughman, *Opt. Commun.* **1999**, *162*, 241.
[188] M. N. Shkunov, Z. V. Vardeny, M. C. DeLong, R. C. Polson, A. A. Zakhidov, R. H. Baughman, *Adv. Funct. Mater.* **2002**, *12*, 21.
[189] N. Eradat, A. Y. Sivachenko, M. E. Raikh, Z. V. Vardeny, A. A. Zakhidov, R. H. Baughman, *Appl. Phys. Lett.* **2002**, *80*, 3491.
[190] K. Sumioka, H. Nagahama, T. Tsutsui, *Appl. Phys. Lett.* **2001**, *78*, 1328.
[191] Z. Z. Gu, S. Hayami, Q. B. Meng, T. Iyoda, A. Fujishima, O. Sato, *J. Am. Chem. Soc.* **2000**, *122*, 10 730.
[192] Z. Z. Gu, A. Fujishima, O. Sato, *J. Am. Chem. Soc.* **2000**, *122*, 12 387.
[193] S. V. Pankova, V. V. Poborchii, V. G. Solovev, *J. Phys.: Condens. Matter* **1996**, *8*, L203.
[194] J. Zhou, C. Q. Sun, K. Pita, Y. L. Lam, Y. Zhou, S. L. Ng, C. H. Kam, L. T. Li, Z. L. Gui, *Appl. Phys. Lett.* **2001**, *78*, 661.
[195] B. G. Kim, K. S. Parikh, G. Ussery, A. Zakhidov, R. H. Baughman, E. Yablonobitch, B. S. Dunn, *Appl. Phys. Lett.* **2002**, *81*, 4440.
[196] I. Soten, H. Miguez, S. M. Yang, S. Petrov, N. Coombs, N. Tetreault, N. Matsuura, H. E. Ruda, G. A. Ozin, *Adv. Funct. Mater.* **2002**, *12*, 71.
[197] D. Y. Wang, F. Caruso, *Adv. Mater.* **2003**, *15*, 205.
[198] A. A. Zakhidov, R. H. Baughman, Z. Iqbal, C. X. Cui, I. Khayrullin, S. O. Dantas, I. Marti, V. G. Ralchenko, *Science* **1998**, *282*, 897.
[199] T. Sumida, Y. Wada, T. Kitamura, S. Yanagida, *Chem. Lett.* **2001**, *31*, 38.
[200] T. Sumida, Y. Wada, T. Kitamura, S. Yanagida, *Chem. Lett.* **2002**, 180.
[201] P. N. Bartlett, T. Dunford, M. A. Ghanem, *J. Mater. Chem.* **2002**, *12*, 3130.
[202] R. W. J. Scott, S. M. Yang, G. Chabanis, N. Coombs, D. E. Williams, G. A. Ozin, *Adv. Mater.* **2001**, *13*, 1468.
[203] J. E. G. J. Wijnhoven, W. L. Vos, *Science* **1998**, *281*, 802.
[204] W. T. Dong, H. Bongard, B. Tesche, F. Marlow, *Adv. Mater.* **2002**, *14*, 1457.
[205] Z. Z. Gu, S. Kubo, W. P. Qian, Y. Einaga, D. A. Tryk, A. Fujishima, O. Sato, *Langmuir* **2001**, *17*, 6751.
[206] D. B. Kuang, A. W. Xu, J. Y. Zhu, H. Q. Liu, B. S. Kang, *New J. Chem.* **2002**, *26*, 819.
[207] S. G. Romanov, A. V. Fokin, R. M. De La Rue, *Appl. Phys. Lett.* **2000**, *76*, 1656.
[208] M. J. A. de Dood, B. Berkhout, C. M. van Kats, A. Polman, A. van Blaaderen, *Chem. Mater.* **2002**, *14*, 2849.
[209] S. Jeon, P. V. Braun, *Chem. Mater.* **2003**, *15*, 1256.
[210] A. Figotin, I. Vitebsky, *Phys. Rev. E* **2001**, *6306*, 066 609.
[211] B. Gates, Y. N. Xia, *Adv. Mater.* **2001**, *13*, 1605.
[212] J. Galloro, M. Ginzburg, H. Miguez, S. M. Yang, N. Coombs, A. Safa-Sefat, J. E. Greedan, I. Manners, G. A. Ozin, *Adv. Funct. Mater.* **2002**, *12*, 382.
[213] E. O. Chi, Y. N. Kim, J. C. Kim, N. H. Hur, *Chem. Mater.* **2003**, *15,* 1929.
[214] C. Koerdt, G. Rikken, E. P. Petrov, *Appl. Phys. Lett.* **2003**, *82*, 1538.
[215] O. D. Velev, P. M. Tessier, A. M. Lenhoff, E. W. Kaler, *Nature* **1999**, *401*, 548.
[216] P. M. Tessier, O. D. Velev, A. T. Kalambur, J. F. Rabolt, A. M. Lenhoff, E. W. Kaler, *J. Am. Chem. Soc.* **2000**, *122*, 9554.
[217] L. B. Xu, W. L. Zhou, M. E. Kozlov, I. I. Khayrullin, I. Udod, A. A. Zakhidov, R. H. Baughman, J. B. Wiley, *J. Am. Chem. Soc.* **2001**, *123*, 763.

[218] P. Jiang, J. Cizeron, J. F. Bertone, V. L. Colvin, *J. Am. Chem. Soc.* **1999**, *121*, 7957.
[219] J. Wijnhoven, S. J. M. Zevenhuizen, M. A. Hendriks, D. Vanmaekelbergh, J. J. Kelly, W. L. Vos, *Adv. Mater.* **2000**, *12*, 888.
[220] L. B. Xu, W. L. L. Zhou, C. Frommen, R. H. Baughman, A. A. Zakhidov, L. Malkinski, J. Q. Wang, J. B. Wiley, *Chem. Commun.* **2000**, 997.
[221] P. N. Bartlett, P. R. Birkin, M. A. Ghanem, *Chem. Commun.* **2000**, 1671.
[222] F. Li, L. B. Xu, W. L. L. Zhou, J. B. He, R. H. Baughman, A. A. Zakhidov, J. B. Wiley, *Adv. Mater.* **2002**, *14*, 1528.
[223] D. J. Norris, Y. A. Vlasov, *Adv. Mater.* **2001**, *13*, 371.
[224] A. Blanco, E. Chomski, S. Grabtchak, M. Ibisate, S. John, S. W. Leonard, C. Lopez, F. Meseguer, H. Miguez, J. P. Mondia, G. A. Ozin, O. Toader, H. M. van Driel, *Nature* **2000**, *405*, 437.
[225] Y. A. Vlasov, X. Z. Bo, J. C. Sturm, D. J. Norris, *Nature* **2001**, *414*, 289.
[226] H. Miguez, S. M. Yang, N. Tetreault, G. A. Ozin, *Adv. Mater.* **2002**, *14*, 1805.
[227] E. Palacios-Lidon, A. Blanco, M. Ibisate, F. Meseguer, C. Lopez, J. Sanchez-Dehesa, *Appl. Phys. Lett.* **2002**, *81*, 4925.
[228] H. Miguez, F. Meseguer, C. Lopez, M. Holgado, G. Andreasen, A. Mifsud, V. Fornes, *Langmuir* **2000**, *16*, 4405.
[229] H. Miguez, E. Chomski, F. Garcia-Santamaria, M. Ibisate, S. John, C. Lopez, F. Meseguer, J. P. Mondia, G. A. Ozin, O. Toader, H. M. van Driel, *Adv. Mater.* **2001**, *13*, 1634.
[230] L. K. van Vugt, A. F. van Driel, R. W. Tjerkstra, L. Bechger, W. L. Vos, D. Vanmaekelbergh, J. J. Kelly, *Chem. Commun.* **2002**, 2054.
[231] F. Garcia-Santamaría, M. Ibisate, I. Rodriguez, F. Meseguer, C. Lopez, *Adv. Mater.* **2003**, *15*, 788.
[232] H. Miguez, A. Blanco, F. Meseguer, C. Lopez, H. M. Yates, M. E. Pemble, V. Fornes, A. Mifsud, *Phys. Rev. B* **1999**, *59*, 1563.
[233] S. G. Romanov, R. M. De la Rue, H. M. Yates, M. E. Pemble, *J. Phys.: Condens. Matter* **2000**, *12*, 339.
[234] Y. C. Lee, T. J. Kuo, C. J. Hsu, Y. W. Su, C. C. Chen, *Langmuir* **2002**, *18*, 9942.
[235] V. Y. Davydov, R. E. Dunin-Borkovski, V. G. Golubev, J. L. Hutchison, N. F. Kartenko, D. A. Kurdyukov, A. B. Pevtsov, N. V. Sharenkova, J. Sloan, L. M. Sorokin, *Semicond. Sci. Technol.* **2001**, *16*, L5.
[236] P. V. Braun, R. W. Zehner, C. A. White, M. K. Weldon, C. Kloc, S. S. Patel, P. Wiltzius, *Adv. Mater.* **2001**, *13*, 721.
[237] V. N. Astratov, V. N. Bogomolov, A. A. Kaplyanskii, A. V. Prokofiev, L. A. Samoilovich, S. M. Samoilovich, Y. A. Vlasov, *Nuovo Cimento Soc. Ital. Fis., D* **1995**, *17*, 1349.
[238] Y. A. Vlasov, N. Yao, D. J. Norris, *Adv. Mater.* **1999**, *11*, 165.
[239] Y. A. Vlasov, K. Luterova, I. Pelant, B. Honerlage, V. N. Astratov, *Appl. Phys. Lett.* **1997**, *71*, 1616.
[240] A. Blanco, C. Lopez, R. Mayoral, H. Miguez, F. Meseguer, A. Mifsud, J. Herrero, *Appl. Phys. Lett.* **1998**, *73*, 1781.
[241] B. H. Juarez, S. Rubio, J. Sanchez-Dehesa, C. Lopez, *Adv. Mater.* **2002**, *14*, 1486.
[242] P. V. Braun, P. Wiltzius, *Nature* **1999**, *402*, 603.
[243] S. G. Romanov, T. Maka, C. M. S. Torres, M. Muller, R. Zentel, *Appl. Phys. Lett.* **2001**, *79*, 731.
[244] B. H. Juarez, M. Ibisate, J. M. Palacios, C. Lopez, *Adv. Mater.* **2003**, *15*, 319.

